GEOLOGICA CARPATHICA, OCTOBER 2018, 69, 5, 498–511 doi: 10.1515/geoca-2018-0029

Integrated stratigraphy of the Upper Barremian–Aptian sediments from the south-eastern Crimea

MARIA S. KARPUK[1, ✉], EKATERINA A. SHCHERBININA[1], EKATERINA A. BROVINA[1], GALINA N. ALEKSANDROVA[1], ANDREY YU. GUZHIKOV[2], ELENA V. SHCHEPETOVA[1] and EKATERINA M. TESAKOVA[1,3]

[1] Geological Institute of RAS, Pyzhevski Lane 7, Moscow, 119017, Russia, ✉maria.s.karpuk@gmail.com
[2] Saratov State University, Department of General Geology and Mineral Resources, Astrakhanskaya st. 83, Saratov, 410012, Russia
[3] Moscow State University, geological department, Vorobiovy Gory 1, Moscow, 123103, Russia

(Manuscript received February 7, 2018; accepted in revised form October 4, 2018)

Abstract: Previous studies made in different parts of the world have shown that Barremian–Aptian times imply many difficulties in deciphering the biostratigraphy, microfossil evolution and correlation of bioevents. In an attempt to improve our knowledge of this period in a particular area of the Tethyan realm, we present the first integrated study of microbiota (including planktonic foraminifera, calcareous nannofossils, ostracods and palynomorphs) and magnetostratigraphy of the upper Barremian–Aptian sediments from south-eastern Crimea. The nannofossils display the classical Tethyan chain of bioevents in this interval, while the planktonic foraminifera demonstrate an incomplete succession of stratigraphically important taxa. Our study enabled the recognition of a series of biostratigraphic units by means of four groups of microfossils correlated to polarity chrons. The detailed analysis of the microfossil distribution led to a biostratigraphic characterization of the Barremian/Aptian transition and brought to light an interval, which may correspond to the OAE1a.

Keywords: Crimea, Barremian, Aptian, biostratigraphy, planktonic foraminifera, calcareous nannofossils, ostracods, palynomorphs, magnetostratigraphy.

Introduction

Thick Lower Cretaceous sediments are widely exposed in south-eastern Crimea southward of the city of Feodosia, where they form the eastern margin of the First Range of the Crimean Mountains. The Berriasian–Valanginian succession, made up of limestones, marlstones and mudstones, gets younger going from the sea-shore cliffs toward the hinterland; these deposits are succeeded by Hauterivian–Aptian non-calcareous and calcareous siliciclastics mostly devoid of or very poor in macrofossils. The Lower Cretaceous sediments of different intervals are studied in this area in varying degrees by different methods, including biostratigraphical, paleomagnetic, sedimentological and geochemical analyses. The main recent studies were focused on the Jurassic/Cretaceous transition (e.g., Arkadiev 2004, 2011; Guzhikov et al. 2012; Arkadiev et al. 2018) and on the upper Berriasian to Valanginian sediments (Arkadiev 2007; Guzhikov et al. 2014; Arkadiev et al. 2017, a.o.). However, during the last half-century the Hauterivian to Aptian sediments of this area were rarely studied (e.g., Salman & Dobrovolskaya 1968; Baraboshkin 2016). In fact, in this area the Hauterivian and most of the Barremian sediments have been disturbed by anthropogenic impact during the last decades and thus are now barely exposed. As a result, we had to limit our study to the upper Barremian–Aptian sediments, which crop out in the Feodosia suburban area.

Recent bio-, magneto- and chemostratigraphic studies dealing with the Barremian–Aptian interval improved calibration of this time period (e.g., Erba et al. 1996; Moullade et al. 1998a,b, 2011; Aguado et al. 1999; Erba et al. 1999; Channell et al. 2000; Ropolo et al. 2008; Coccioni et al. 2012; Savian et al. 2016, a.o.). The base (GSSP) of the Aptian stage is not yet formally ratified, however, the base of M0 Magnetochron has been considered by many authors to define the Barremian/Aptian boundary since the proposition of the Aptian Working Group in 1996 (Erba et al. 1996). The classical biostratigraphy of this interval in the Tethyan realm includes ammonite and planktonic foraminifera (PF) zonations, which are still in progress mainly because of problems of correlation between the Tethyan and Boreal Realms, and standard nannofossil zonations codified with CC (Sissingh 1977) and NC (Roth 1978; Bralower et al. 1995) labels. Ammonites are scarce or absent from the upper Barremian to Aptian of the Crimea and thus could not be used in the biostratigraphy of this interval in the studied area.

A developed micropaleontological study of the Lower Cretaceous sediments in Crimea began in the second half of the last century. The occurrence of abundant and diverse calcareous nannofossils in the Crimean Lower Cretaceous was shown by Vishnevsky & Menaylenko (1963) and Shumenko (1974), but they did not consider the possibility of their stratigraphic application. The study of the Barremian–Aptian stratigraphic division based on PF was pioneered by T.N. Gorbachik (Gorbachik 1959, 1964, 1969, 1986; Gorbachik & Krechmar 1969). This author proposed the zonal subdivision of

the Barremian–Aptian sediments on the basis of PF study in the south-western Crimean sections (Fig. 1).

Recently, new research has been carried out towards a more detailed subdivision and correlation of the Lower Cretaceous sediments from south-western and central Crimea. Calcareous nannofossil studies processed on several Lower Cretaceous sections in south-western Crimea enabled their detailed subdivision following the CC and NC standard zonations (Shcherbinina & Loginov 2012). The classical sections described by T.N. Gorbachik were revisited and PF assemblages were restudied (see Brovina 2017 and discussion herein; Brovina et al. 2017) to improve the correlation of the Crimean upper Barremian–Aptian subdivisions with the Tethyan PF zonation.

The Crimean Barremian–Aptian ostracods were first found and described by T.N. Nemirovskaya (1972), but without stratigraphical analysis. Several decades later, Karpuk (Karpuk & Tesakova 2010, 2013, 2014; Karpuk 2016a,b) studied the species composition, stratigraphical distribution and paleoecological affinities of the Barremian–Aptian ostracods of the Crimean Mts. The succession of four ostracod zones was established in this interval and correlated to the PF and calcareous nannofossil zonation (Brovina et al. 2017). The preliminary study of dinocysts in SW Crimea led to the identification of two dinocyst assemblages in the uppermost Barremian and lowermost Aptian (Shurekova 2016). In the 2000s, paleomagnetic studies of the Lower Cretaceous defined the position of the M0 Chron in SW Crimea (Baraboshkin et al. 2004; Yampolskaya et al. 2006), but magnetostratigraphy of this interval from E Crimea was not initiated up to now.

This paper presents the first study of the upper Barremian to Aptian sediments of the Zavodskaya Balka section, south-eastern Crimea. This work includes the stratigraphic distribution of planktonic foraminifera, calcareous nannofossils, ostracods, palynomorphs and magnetostratigraphy. The obtained results enabled the first stratigraphic subdivision of the succession and correlation of the bioevents recognized among the different groups of microfossils.

Material and methods

Material

The outcrop of Zavodskaya Balka was studied and sampled in the upper SE part of the ravine crossing the eastern wall of the abandoned quarry located 1 km eastward from the city of Feodosia, on the left side of Feodosia–Ordzhonikidze road (GPS data: 45°1'56" N, 35°20'14" E; Fig. 2). The 33.5 m-thick mid-Cretaceous muddy succession (dip azimuth — 50°, dip angle — 20°) with decimetre-scale intercalations of carbonate and hard ferruginous beds was first sampled using nearly equal intervals (1.3–1.5 m). 23 samples were collected and on the basis of a preliminary study, a few additional samples were taken during a recent field trip from two particular intervals: one which was suggested to include the OAE1a (between 15.0 and 19.0 m) and another — the Barremian/Aptian boundary (between 5.3 and 9.0 m). The Barremian–Aptian succession in the Zavodskaya Balka section consists of light grey mudstones and contains irregularly intercalated reddish layers. The calcium carbonate content varies throughout the section from 3.92 to 42.85 %. The $CaCO_3$ mainly comes from coccoliths, foraminiferal tests, ostracod valves and carapaces and rare fragments of macrofossils. The sediment is intensively bioturbated mostly by small burrows (up to 0.5 mm in diameter and few mm in length). The harder intercalations consist of diagenetic limestone and marlstone concretions made of microcrystalline calcite aggregates. Some of these beds can be interpreted as hardgrounds formed during a process of non-deposition. They contain manganocalcite, siderite and phosphatic matter (apatite) (Fig. 3). The TOC content is very low in the whole succession and irregularly varies between 0.5 and 1.2 %.

Methods

All the samples obtained were processed for paleomagnetic and micropaleontological analyses using the following methods.

Calcareous nannofossils: Smear-slides for nannofossil study were prepared from raw sediment with Norland Optical Adhesive 61 using standard techniques (Bown & Young 1998). Nannofossils were examined at 1250x magnification under light microscope Olympus BX41 and their pictures were made using an Unfinity X video-camera.

Planktonic foraminifera and ostracods: The sample preparation evolved from the technique described by Sohn (1961). All ostracod specimens from the 0.1–1 mm fraction were picked. All PF specimens were picked up from the samples with rare PF and only the first hundred specimens from the samples rich in PF. Ostracods and PF images were made using the CamScan Electron Microscope of the Paleontological Institute of the Russian Academy of Sciences.

Palynomorphs were studied from 12 samples (23, 19, 17, 15, 14, 13, 1504, 10, 8, 6, 3, 1). Chemical preparation of samples for palynological study followed the method developed by the research team of the Geological Institute of the RAS (see, for example, Shcherbinina et al. 2016). Spores, pollen and microphytoplankton (dinoflagilates, algae) were examined at 400–600× magnification under a light microscope Carl Zeiss Axioplan and their pictures were made using a Canon PowerShot A640 camera and an Axiovision visualization programme. Two hundred specimens were counted from samples with abundant palynomophs and all specimens from the samples with less rich palynomophs.

Magnetostratigraphy: The field and laboratory rock-magnetism and paleomagnetic studies and data processing were carried out by standard procedures (Khramov 1982). Oriented samples were sawn up into 3 to 4 cubes with 2 cm-long sides. They were treated with magnetic cleaning by variable field using LDA-3 AF C outfit under the temperature obtained using the kiln designed by V.P. Aparin. The Lab Petromagnetic and magneto-mineralogical analysis includes: magnetic

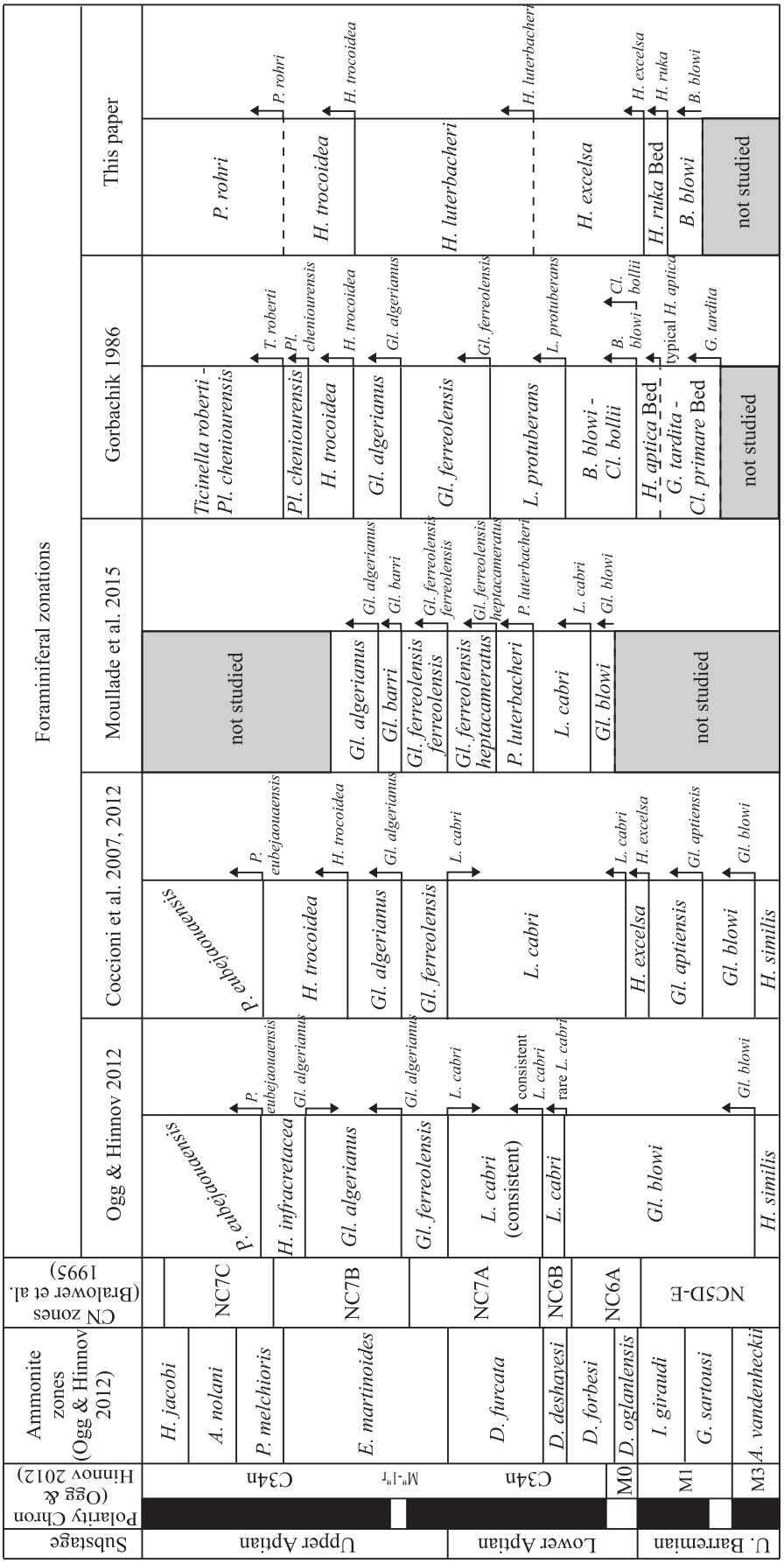

Fig. 1. Tethyan late Barremian–Aptian standard stratigraphy and PF zonations of different authors. Correlation of ammonite and nannofossil zonations after Bown et al. 1998; Aguado et al. 1999; Szives et al. 2018.

susceptibility (K) and its anisotropy (AMS) measurements, experiments with magnetic saturation, differential thermomagnetic analysis (DTMA). $\mathbf{J_n}$ measuring was done using spinner magnetometer JR-6, K — on kappabridge MFK-1FB. The faction thermoanalyser TAF-2 was used for DTMA. Analysis of the data on AMS and the component analysis were performed using, respectively, Anisoft 4.2 and Remasoft 3.0 software. 32 samples were processed from the complete succession.

Results

Magnetostratigraphy

One or several similarly oriented components of normal geomagnetic polarity (N) were defined in all samples with the sole exception of sample 19 in which the characteristic remanent magnetization (**ChRM**) cannot be confidently defined. However, the projection of the paleomagnetic vector regularly becomes displaced during magnetic cleanings along the arc of the great circle from the lower to upper hemisphere.

Rock magnetic and mineralogical study: As shown by differential thermomagnetic analysis (DTMA) curves, magnetite is the major source of magnetization in the grey mudstones of the lower part of the section. This is determined by the drop of magnetization near — 578 ºC, that is the Curie temperature of this mineral (Fig. 4A–I). $FeCO_3$ is detected by the increased magnetization at 350 °C due to the phase transition of siderite into magnetite in the samples from siderite concretions and red beds. During the second

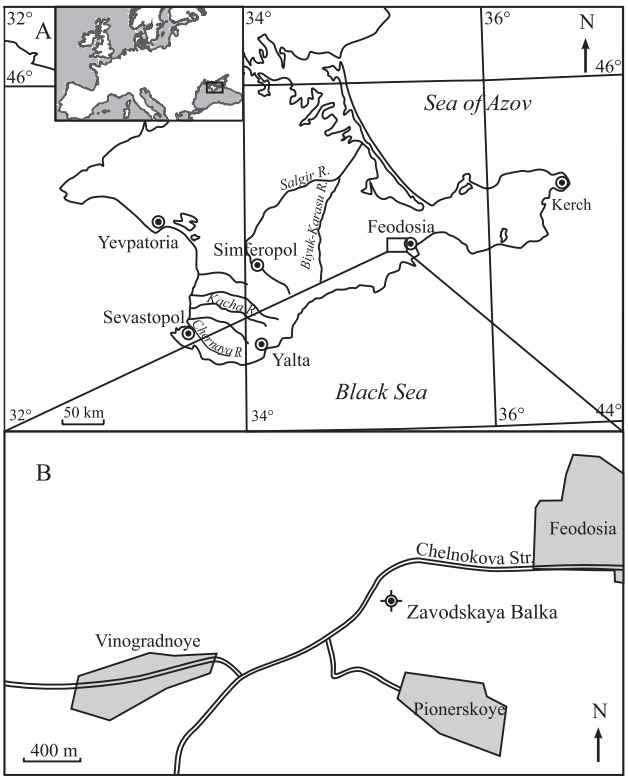

Fig. 2. Location of the studied section in the general geography (**A**) and the sketch-map of the vicinity of the city of Feodosia (**B**).

heating, magnetite becomes the only magnetic mineral left (Fig. 4A-II).

The effect of Fe hydroxides, such as hydrogoethite (peak around 100–150 ºC on the second derivative), on thermomagnetic curves is negligible (Fig. 4A-I). However, the magnetic saturation curves demonstrate a magnetically rigid phase, featured for ferric oxides, in the red sediments of sample 8. This is proved by non-saturation in the high fields (up to 700 mT; Fig. 4B-I). In all other samples (Fig. 4B-II), mainly the magnetically soft phase, featured for the fine magnetite, is detected.

The average values of K and $\mathbf{J_n}$ in the grey mudstones are $66*10^{-5}$ of SI units and $23*10^{-3}$ A/m, respectively, which indicates high concentrations of magnetite (Fig. 3). The samples rich in siderite are characterized by abnormally high values of $\mathbf{J_n}$ — 179–$1080*10^{-3}$ A/m (Fig. 3) and nearly reversed magnetic fabric with the long axes projections of the magnetic ellipsoids (K1) approaching the centre of stereoprojection (Fig. 4C-I). The AMS in the grey mudstones tends towards classic sedimentary magnetic fabric, where short axes (K3) are vertical and K1 projections lie along the stereogram margin (Fig. 4C-II). The ranking of the long axes of the magnetic ellipsoids along the NW–SE direction (Fig. 4C-II) is similar to the arrangement of K1 in the studied earlier Berriassian mudstones that outcrop 1 km east of the studied section (Guzhikov et al. 2014; Fig. 4C-III). The similarity of this parameter throughout the whole territory of the Crimean Mts. is likely to be caused by large-scale tectonic compression (Bagaeva & Guzhikov 2014). The shape of the magnetic particles is defined from the Flinn diagram (Flinn 1965; Fig. 4C). Both elongated and flattened forms of the magnetic ellipsoids are characteristic for samples containing siderite (Fig. 4C-I); the flattened form of the magnetic ellipsoids dominates in other mudstones (Fig. 4C-II). This is likely to be related to the aggregation of sub-micrometer sized ferromagnetic grains on the flakes of clay minerals.

The age determination of magnetization components, associated with siderite or iron hydroxides, is difficult or invalid because the components are more likely to be of the chemical genesis. The samples containing these minerals, marked by anomalously high $\mathbf{J_n}$ values ($>100*10^{-3}$ A/m; Fig. 3), should be excluded from consideration. This does not imply significant variations in the structure of the paleomagnetic column.

Paleomagnetic study: All magnetization components are defined with high accuracy (maximal angle of deviation (MAD) is less than 10°). Only one magnetization component $\mathbf{C_1}$ is determined in some samples (Fig. 5A-I). Both low-coercivity or low-temperature component ($\mathbf{C_L}$) and high-coercivity or high-temperature characteristic component magnetization (**ChRM**) are recognized in most of the samples (Fig. 5A-II). The projections of all components ($\mathbf{C_1}$, $\mathbf{C_L}$ and **ChRM**) are located in the northern rhumbs of the lower hemisphere (Fig. 5B) that characterizes the magnetization of normal polarity.

A different pattern of the paleomagnetic vectors is observed during magnetic cleanings of sediments sampled between the levels 3129-3 and 3129-9: the $\mathbf{J_n}$ projections displace along the arcs of the great circles (GC; Fig. 5C). Not less than 4 (mainly 5–8) points were used for the approximation of the tracks of the changing $\mathbf{J_n}$ directions during the magnetic cleanings (the MAD is less than 10°).

Dating of paleomagnetic components: In the single-component samples, the mean $\mathbf{C_1}$ vector has normal polarity direction and corresponds to the magnetic inclination near the city of Feodosia (I=63.4°; Fig. 5-I). More likely, the sediments of these intervals were completely remagnetized by the present-day geomagnetic field, and $\mathbf{C_1}$ is a viscuous remanent magnetization (VRM). In the two-component samples, the mean $\mathbf{C_L}$ and $\mathbf{C_1}$ vectors statistically coincide (Fig. 5B-I, II, IV), while the mean direction of **ChRM** and $\mathbf{C_1}$ (and **ChRM** and $\mathbf{C_L}$) significantly differ (Fig. 5B-I–IV). This pattern is in good accordance with the hypothesis of the secondary (viscous) nature of the $\mathbf{C_L}$ and $\mathbf{C_1}$ components, related to the modern magnetic field, and primary nature of the ChRM component.

The regular displacement of the $\mathbf{J_n}$ projections along the arcs of GC from lower to upper hemisphere is featured for reversely magnetized deposits, which were partially remagnetized by the modern magnetic field. The recognition of the zones of reverse polarity in the paleomagnetic column of the section (Fig. 3) is based on the suggestion that the presence of the ancient reverse polarity component caused the displacement of the paleomagnetic vectors along the arcs of great circles.

Since the primary $\mathbf{J_n}$ components were not reliably identified, their orientational and/or chemical genesis is still poorly

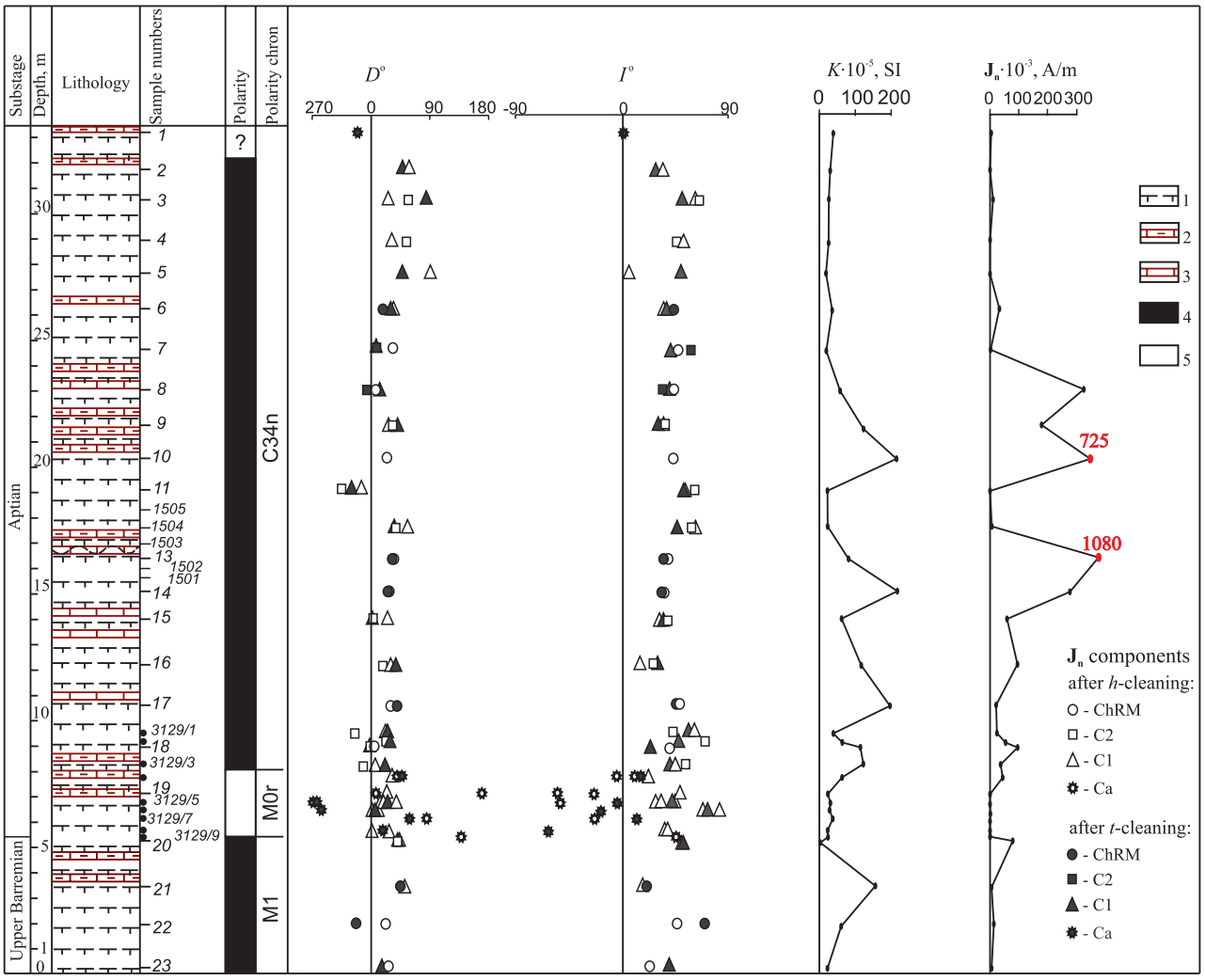

Fig. 3. Magnetostratigraphic characteristics of the Barremian–Aptian sediments of the Zavodskaya Balka section. D, I — palaeomagnetic declination and inclination, respectively; K — magnetic susceptibility; $\mathbf{J_n}$ — natural remanent magnetization. Symbols: 1 — calcareous mudstones, 2 — diagenetic concretions of limestones and marlstones, 3 — beds containing manganocalcite, siderite and, sometimes, impure of phosphatic matter, 4 — normal polarity, 5 — reverse polarity.

understood and standard field tests and other criteria elaborated by different researchers for estimation of the validity of the paleomagnetic results cannot be used. Nevertheless, the biostratigraphic age determination, detailed sampling and thorough magnetic cleanings caused reliable values of the index of paleomagnetic consistency of the results obtained: 5 from 10 using Opdyke and Channell's method (1996) and 3 from 7 using Van der Voo's method (1993). Since the M0 Chron is the unique interval with reversed polarity at the Barremian/Aptian transition (Ogg et al. 2016), the reverse polarity zone found between samples 3129/9 and 3129/3 is, more likely, its analogue and the associated Barremian–Aptian boundary can be assigned at the level of the sample 3129/9.

Planktonic Foraminifera

The numerous researches published since the 1960-s in different Tethyan areas enabled the detailed zonal subdivision of the late Barremian to Aptian interval (Moullade 1966, 1974; Gorbachik 1986; Moullade et al. 1998a,b, 2005, 2015; Risch 1971; Coccioni et al. 2007, a.o.; Fig. 1). Our study of PF from the Zavodskaya Balka section led to identification of the levels of zonal markers used in zonations of Moullade et al. (2011, 2015), Coccioni et al. (2007) and GTS (Ogg & Hinnov 2012). *H. trocoidea* Zone is defined here *sensu* Moullade (1966), that was used later by Gorbachik (1986) in the Crimea and thus falls within the interval, which corresponds to the *H. infracretacea* Zone of Ogg & Hinnov (2012).

The PF assemblages of the studied succession show significant variations in total abundance, species diversity and planktonic/benthic (P/B) ratio. A total of 15 species are identified in the whole succession (Table S1). *Hedbergella infracretacea* (Glaessner, 1937) dominates the PF assemblage throughout the section. The total abundance widely varies, increasing above the level of sample 16 (12.2 m) and dropping dramatically above sample 6 (26.3 m). The species diversity

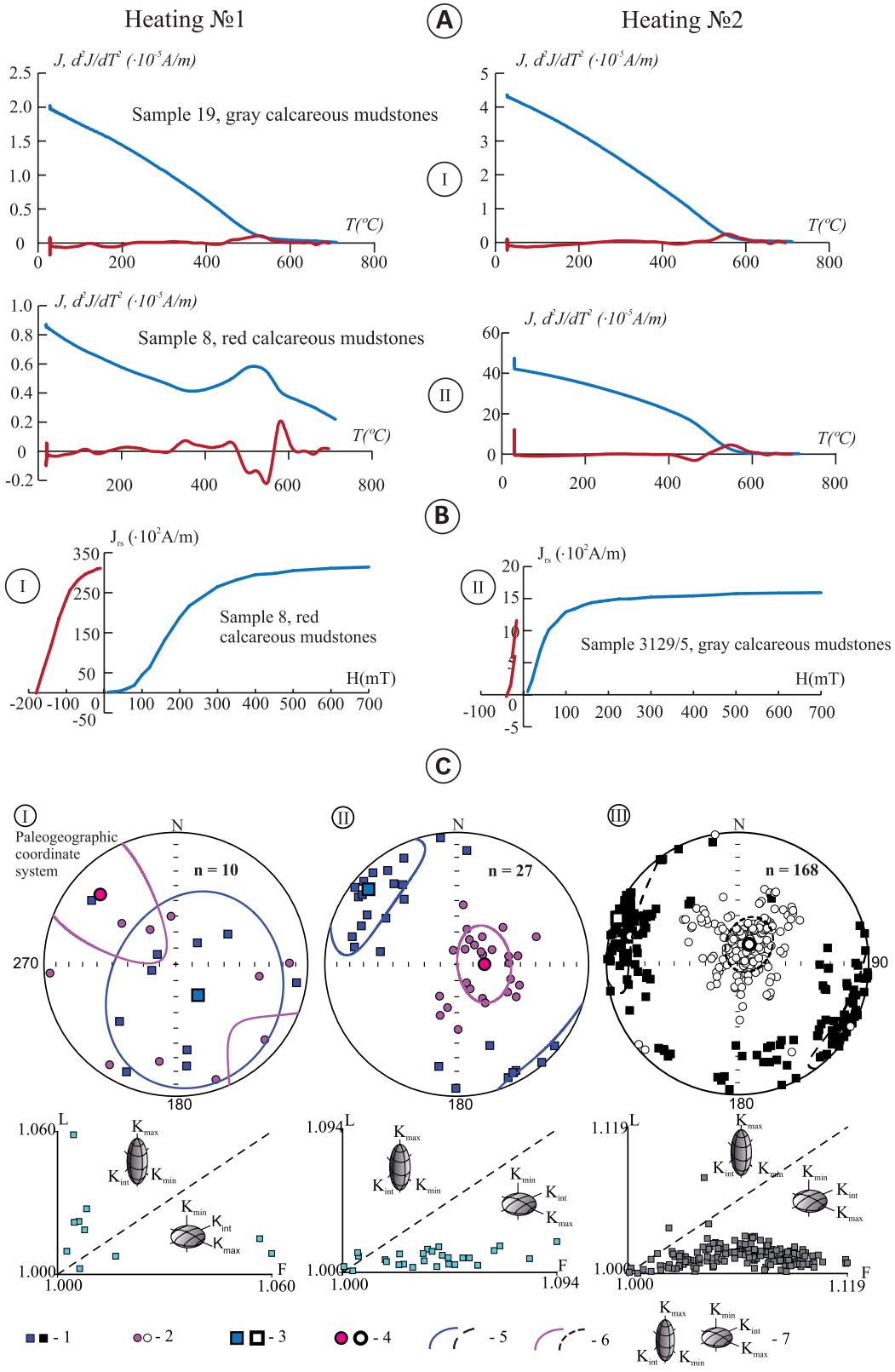

Fig. 4. The results of magnetic and mineralogical analysis: **A** — DTMA curves from the first and the second heatings: thermomagnetic curves (blue (black) colour) and second-order derivatives from them (red (grey) colour); **B** – magnetic saturation plots; **C** — anisotropy of the magnetic susceptibility characteristics (distribution of projections of AMS ellipsoid axes over the sphere in the paleogeographic coordinate system and the relationship of L and F parameters, n — the number of samples in a set): **I**, **II** — samples with siderite and grey clays in the studied section; **III** — grey carbonate clays in the upper Berriasian from the Zavodskaya Balka section (Guzhikov et al. 2014). Symbols: 1, 2 — long (K1) and short (K3) axes of AMS ellipsoids, respectively; 3, 4 — average values for K1 and K3, respectively; 5, 6 — confidence ellipse for K1 and K3, respectively; 7 — sketch of the AMS ellipsoid forms.

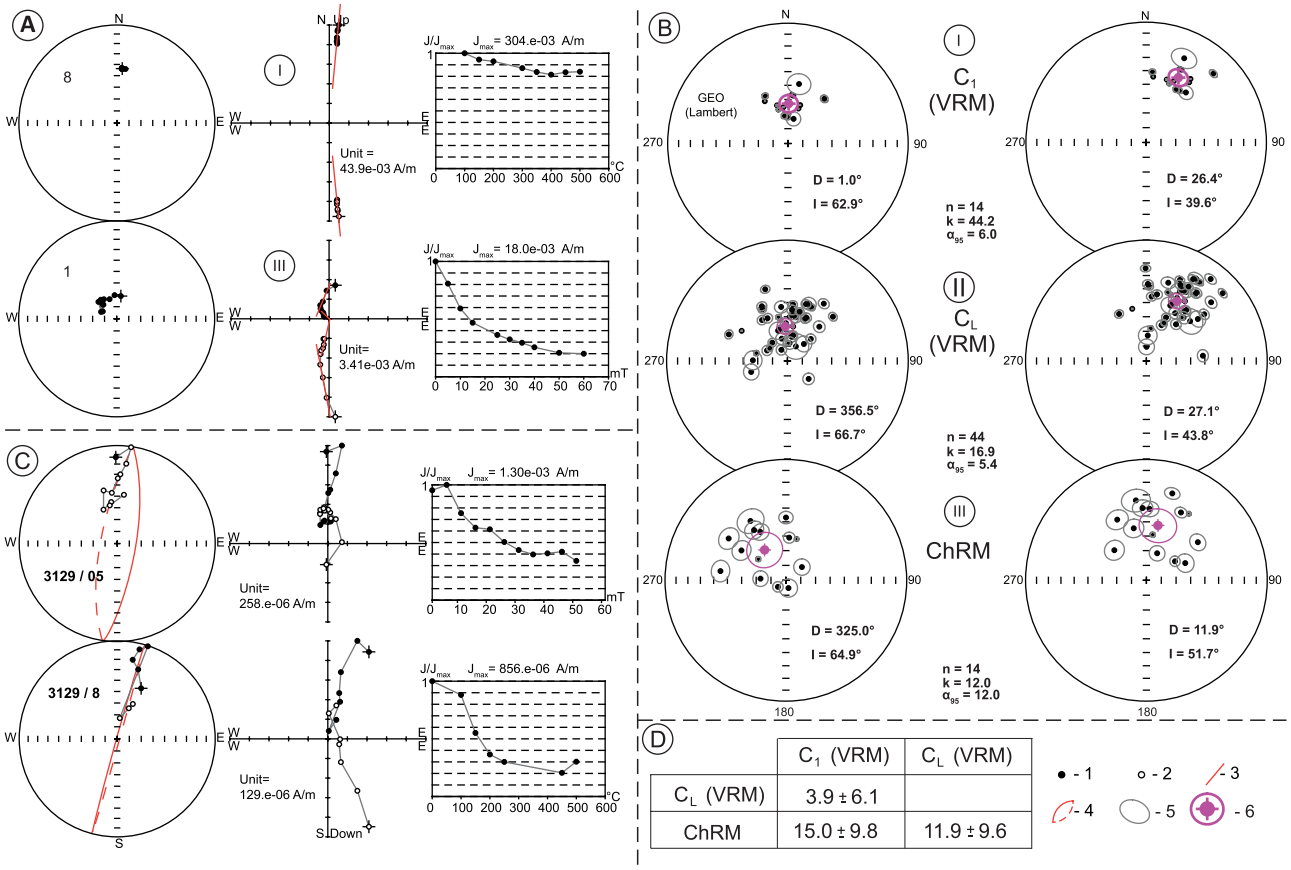

Fig. 5. The results of the magnetic component analysis: **A** and **C** (from left to right) — stereographic presentation of $\mathbf{J_n}$ changes in the process of magnetic cleaning, Ziderweld diagrams, sample demagnetization plots (I — single-component sample, II — two-component sample); **B** — stereographic projection of $\mathbf{J_n}$ components before (left) and after (right) tectonic correction: $\mathbf{C_1}$ **(VRM)** (I), $\mathbf{C_L}$ **(VRM)** (II), **ChRM** (III) (D_{av}, I_{av} — average paleomagnetic declination and inclination, respectively, n — number of samples in a set, k — interbedded paleomagnetic precision parameter, $\boldsymbol{\alpha_{95}}$ — radius of the vector confidence circle); **D** — angles formed by mean directions of **ChRM**, $\mathbf{C_1}$, $\mathbf{C_L}$. The angles between paleomagnetic vectors are given with inaccuracy (±) determined by the statistics of these vectors according to Debiche & Watson 1995. If the angle is greater than the inaccuracy, the vectors differ greatly. If the angle is smaller than the inaccuracy, the vectors statistically match (Debiche & Watson 1995). Legend: 1, 2 — $\mathbf{J_n}$ projections on the lower semisphere and the upper semisphere, respectively; 3 — line segments corresponding to the $\mathbf{J_n}$ components; 4 — great circles; 5 — MAD for each component, 6 — average direction of $\mathbf{J_n}$ components with confidence circle, 7 — direction determined by GC intersection with confidence circle.

gradually increases from two species in the lower part of the section (0–7.0 m, samples 23–19) to 9 species in the middle of the section (17.0–18.3 m, samples 1503–1505), with a small decrease between 14.0 and 16.5 m (samples 15–13). The interval between samples 10 and 6 (20.2–26.3 m) is characterized by the occurrence of abundant *H. infracretacea*, together with rare *H. trocoidea* (Gandolfi, 1942) in the restricted interval of 21.8–23 m. Poor and low-diversity PF assemblages are found in the uppermost part of the section.

We identified six PF zones in the studied succession. The *Blowiella blowi* Zone is defined in the lower part of the section (samples 23–18) by the occurrence of the index species (Fig. 6). We should emphasize that we accept the view suggesting the differentiation of two genera: *Blowiella* Kretchmar and Gorbachik, 1971 and *Globigerinelloides* Cushman and ten Dam, 1948. According to this concept, *Blowiella* specimens have smooth planispiral tests mainly with few chambers (up to 5), while *Globigerinelloides* usually have more chambers (>6) and coarser sculpture (for more detailed taxonomic discussion see Brovina 2017).

The successive FOs of *Hedbergella ruka* (Banner, Copestake and White, 1993) and *Hedbergella excelsa* Longoria, 1974 (in samples 18 and 17, respectively) are very characteristic in many Crimean sections (Brovina 2017). This enabled us to establish the *H. ruka* Bed[1] in the lowermost Aptian. The FO of *H. excelsa* marks the base of an overlying zone (Coccioni et al. 2007). It should be mentioned that the stratigraphic range of this zone in the studied section differs from the *H. excelsa* Zone of Coccioni et al. (2007), where it ranges from the latest Barremian to the earliest Aptian, while the FO of the marker is shown in the *Deshayesites weissi* ammonite Zone (=*Des. forbesi* Zone according to Reboulet et al. 2014), which means

[1]According to the Russian Stratigraphic Code, a faunistic Layer or Bed is an informal biostratigraphic unit, which is characterized by a specific fossil assemblage, but is inconsistent with any type of biozone, because its boundaries cannot be clearly defined by any reasons.

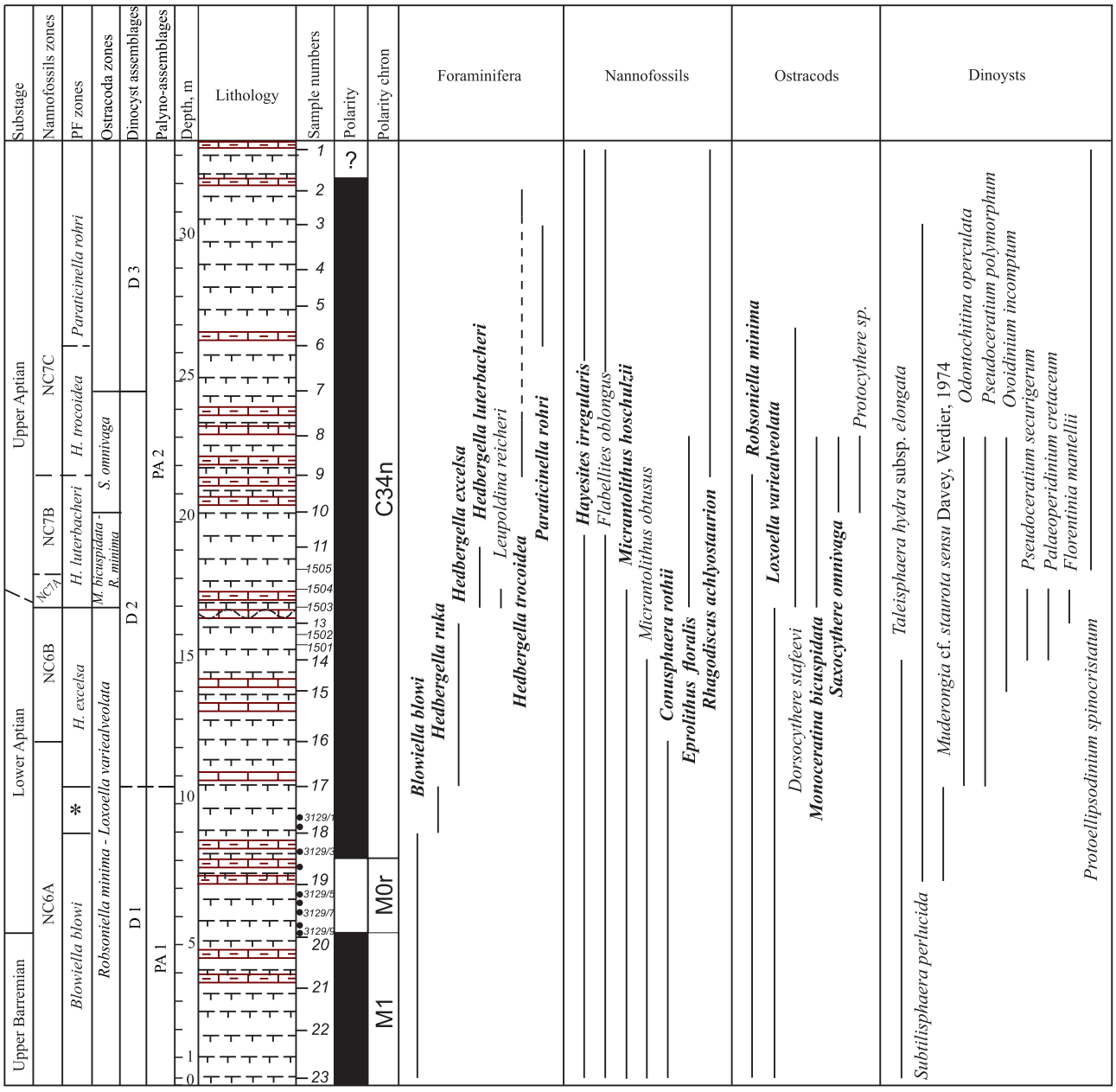

∗ - *H. ruka* Bed

Fig. 6. The bio- and magnetostratigraphy and the stratigraphic ranges of the main markers of PF, nannofossils, ostracods and dinocysts of the Zavodskaya Balka section. Zonal markers are shown in bold.

above the interval of the *H. excelsa* Zone (Coccioni et al. 2007: fig. 2, p. 217). In the Zavodskaya Balka section, the FO of this species is found in the early Aptian, on the basis of the paleomagnetic results, which lead us to assume that the Barremian/Aptian boundary is close to sample 19 (see above). The absence of stratigraphically important species in the interval between samples 17 and 1503, lower than the FO of *Hedbergella luterbacheri* Longoria, 1974, caused the larger stratigraphic interval of *H. excelsa* Zone in the studied section, which covers the lower part of *Leupoldina cabri* Zone of Coccioni et al. (2007). The non-occurrence of *L. cabri* (Sigal, 1952) in the Zavodskaya Balka section can be caused by both ecological factors and/or the hiatus between samples 13 and 1503. The FO of *H. luterbacheri* in the sample 1503 marks the base of the eponym zone and this species disappears in the sample 1505. Although the FO of *H. luterbacheri* is found much earlier in Spain (lower Barremian) by Coccioni et al. 2007, the level of its FO in France and Crimea is likely isochronous and this provides a good reason to distinguish here the *H. luterbacheri* Zone as defined by Moullade et al. (2015).

In the overlying interval of the outcrop (18.5–21.5 m, samples 11–10), the usual PF Tethyan markers were not found. Above (sample 9, 21.5 m), the FO of *Hedbergella trocoidea* marks the base of the eponym zone. As a result, all zones

based on the well-known *Globigerinelloides* phyletic lineage (*Gl. ferreolensis heptacameratus* Moullade et al., 2008, *Gl. ferreolensis ferreolensis* (Moullade, 1961), *Gl. barri* (Bolli, Loeblich and Tappan, 1957), *Gl. algerianus* Cushman and ten Dam, 1948) used in the zonation of Moullade et al. (2015) cannot be applied here due to the absence of these species in the studied succession. The absence of these multichambered species, assumed to be deeper water dwellers (Leckie 1987) might be caused by the low paleodepth of the SE Crimean basin.

Despite the diachroneity in the FO of *H. trocoidea* in many areas (Spain: in *Gl. ferreolensis* Zone (Coccioni et al. 2007); South France: in *Gl. algerianus* Zone (Moullade 1966); Bavarian calcareous Alps: uppermost Aptian (Risch 1971) a.o.), this bioevent seems to be the useful regional zonal marker for the Crimea, as was already shown by previous studies (Gorbachik 1986; Brovina 2017).

The specimens with few (5–6) chambers in the last whorl, coalesced perforation cones and cover-plates (Supplementary Fig. S1:19–22) found in Zavodskaya Balka section can be attributed to *Paraticinella rohri* according to the species definition given by Premoli Silva et al. (2009): "umbilical area is covered by large flaps from the ultimate and penultimate chambers that form a cover-plate", while the inner whorl of *Hedbergella* is always exposed. We consider these tests as *Pt. rohri* juveniles, as there are only 5–6 chambers, while adult *Pt. rohri* have 9 chambers in the last whorl. The FO of these specimens in sample 6 (25.3 m) is considered here as the base of the eponym zone. The rare adult specimens of *Pt. rohri* are found at the higher level (sample 4, 29.0 m).

In the uppermost part of the outcrop (samples 3–1, 30.8–33.2 m), PF are very rare and agglutinated benthics widely dominate the foraminiferal assemblage. Based on a previous study (Gorbachik 1986), such an assemblage likely corresponds to the lower Albian interval; however, we have no other indication for an Albian age of this part of the section.

Calcareous nannofossils

The calcareous nannofossils of the Zavodskaya Balka section show moderate to good preservation and significant fluctuations in both total abundance and species diversity. Different species of *Watznaueria* largely dominate the assemblages in the whole studied interval. The warm-water *Rhagodiscus* are common, showing minor variations in relative abundance. In addition, generally rare specimens of *Zeugrhabdotus*, *Flabellites oblongus* and cool-water *Assipetra* permanently occur in most of the succession (Supplementary Figs. S2, S3, Table S2).

The more abundant and diverse nannofossil assemblage is found in the lower part of the succession (0–14 m, samples 23–15), where it includes *Micrantholithus obtusus* Stradner, 1963, *M. hoschulzii* (Reinhardt, 1966), *Conusphaera rothii* (Thierstein, 1971), *Hayesites irregularis* (Thierstein *in* Roth & Thierstein, 1972) and common nannoconids. Nannofossils dramatically reduce their abundance and species diversity at the level of 15.0 m (sample 14) and disappear in the short interval comprising samples 1501–1502 (15.5–16.0 m). Above this interval, nannofossil abundance and species diversity progressively increase again, but without attaining their former representativity. The upper part of the section contains only rare nannofossil specimens, which dramatically decline at 29.0 m (sample 4), but then slightly recover at 33.2 m.

Several nannofossil bioevents were identified in the studied succession. The occurrence of *Hayesites irregularis* at the very base of the section suggests that this interval belongs to the NC6A Subzone (Fig. 6). In many areas worldwide, the FO of *H. irregularis* is documented prior to the base of magnetic Chron M0 (e.g., Channell et al. 2000; Ogg & Hinnov 2012; Patruno et al. 2015, a.o.). In the Zavodskaya Balka section, this species occurs at least at 7.0 m below the Chron M0. The nannofossil assemblage of NC6A Subzone is distinguished by common and diverse nannoconids, which dramatically decline at the top of this subzone interval (sample 16, 12.2 m, Fig. 7). Such nannoconid decline evidently corresponds to widely known events named "nannoconid crises", preceding the global Oceanic Anoxic Event 1a (OAE1a; Erba 1994; Aguado et al. 1999; Erba et al. 1999; Habermann &

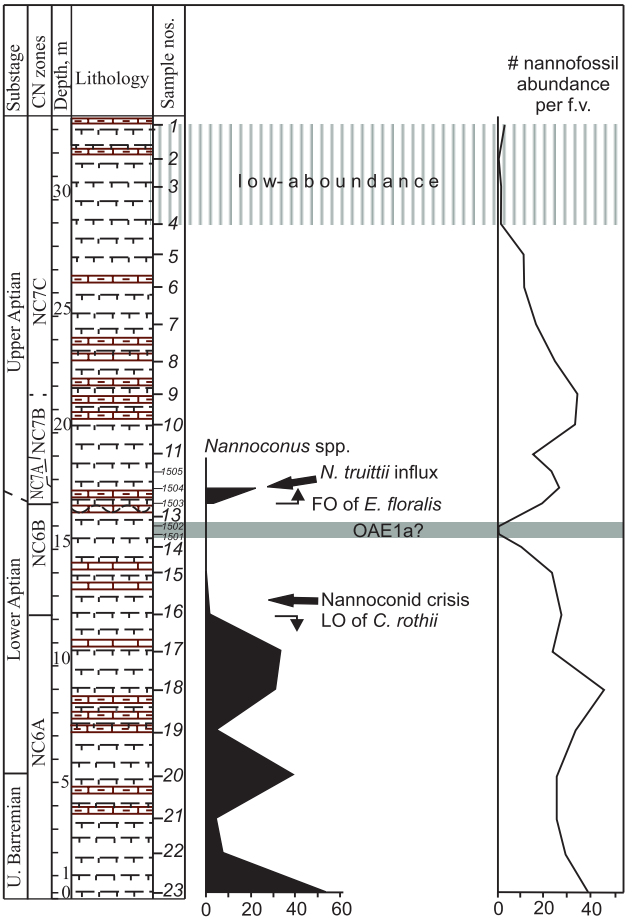

Fig. 7. Upper Barremian to Aptian nannofossil bioevents in the Zavodskaya Balka section.

Mutterlose 1999; Erba & Tremolada 2004; Luciani et al. 2006; Bottini et al. 2015).

The LO of *Conusphaera rothii* in the sample 15 (14.0 m) marks the base of the NC6B Subzone (Roth 1978; Bralower et al. 1995). The nannofossil abundance tends to impoverish toward the middle of this subzone and the interval 15.5–16.0 m (samples 1501–1502) is even nannofossil-free. This interval is made up of non-calcareous mudstone and might correspond to OAE1a. However, this assumption needs much more evidence (e.g., stable isotope analyses) because of low contents of both TOC and $CaCO_3$ at this level. The FO of *Eprolithus floralis* (Stradner, 1962) is found above this interval at the level 17.0 m (sample 1503); this event corresponds to the base of the NC7 Zone (Roth 1978; Bralower et al. 1995). The division of this interval into subzones is quite difficult, since the LO of *M. hoschulzii*, which defines the base of the NC7B Subzone, is documented much earlier in the Crimea — in the NC6A Subzone (E. Shcherbinina, personal observations). Although few specimens of this species are found in sample 1504 (~17.5 m, bottom of NC7 Zone) in the Zavodskaya Balka section, the inconsistent occurrence of M. *hoschulzii* in the section and the diachronicity of its LO in the area make the location of this boundary rather tentative. The short-time re-occurrence of rare nannoconids at the level of 17.5 m (sample 1504) likely corresponds to the episode of "nannoconid abundance pulse" documented in Italy (Patruno et al. 2015). The FO of typical *Rhagodiscus achlyostaurion* (Hill, 1976) (small *Rhagodiscus* with bright birefringent spine filling the central area) is found at the level of 21.5 m (sample 9), which can suggest the base of the NC7C Subzone. However, similar specimens with smaller spine occur earlier in some sections of the Crimea (Brovina et al. 2017), in the lower part of NC7 Zone, and equivocation of problems in the definition of this species also leads to some uncertainty on the recognition of its FO.

Ostracoda

Ostracod assemblages show an uneven distribution throughout the section. Their total abundance and species diversity are relatively high in the lower part of the succession (0–12.5 m, sample 23–16). Their abundance progressively decreases at the level 14.2 m (sample 15) up to a total elimination in the interval 15.2–16.0 m (samples 14–1502). Above this interval, the ostracod amount is restored between 16.0–21.5 m (samples 1503–9), but it never reaches its former abundance and finally declines in the interval 30.5–33.5 m (samples 3–1) (Supplementary Fig. S4, Table S3). The species composition of Lower Cretaceous ostracod assemblages of Crimea appears to be affected by a marked endemism and thus none of the proposed zonations (Neale 1978; Wilkinson & Morter 1981; Damotte et al. 1981; Babinot et al. 1985; Lott et al. 1985, 1986; Wilkinson 1988, 2008; Vivers et al. 2000; Woods et al. 2001; Coimbra et al. 2002; Bachmann et al. 2003) can be applied in this area. Nevertheless, the recent study of ostracod stratigraphic distribution in the upper Barremian–Aptian sediments of the SW Crimea enabled the recognition of several correlative ostracod Zones (Karpuk 2016b; Brovina et al. 2017), which were also found in the Zavodskaya Balka section.

The diverse assemblage of the lower part of section (samples 23 to 15) includes up to 35 species. The co-occurrence *Loxoella variealveolata* Kuznetsova, 1956 and *Robsoniella minima* Kuznetsova, 1961 allows the identification in this section of the *L. variealveolata–R. minima* Zone of Karpuk (2016b) (Fig. 6).

Several eurybiontic species, such as different cytherellas, *Bairdia projecta*, *Bythocypris* sp., *Cytheropteron ventriosum*, reappear at the level of sample 1503, but with few specimens. *Monoceratina bicuspidata* (Gründel, 1964) and *Dorsocythere stafeevi* Karpuk et Tesakova, 2013 show their FOs at this level and they gradually tend to dominate the assemblage along with *R. minima*, which disappears above sample 9 (16.5 m). The FO of *M. bicuspidata* corresponds to the base of the *M. bicuspidata–R. minima* Zone, which is defined by the co-occurrence of these two species. The FO of *Saxocythere omnivaga* (Lyubimova, 1965) in sample 10 (~20.5 m) marks the base of the *S. omnivaga* Zone, where this species represents its most characteristic feature. *Protocythere* sp. is an additional marker of this zone, because it becomes common in this interval and co-occurs with *S. omnivaga* in many sections studied in Crimea (Karpuk 2016b). Above the level ~24.5 m (sample 7), many ostracod species become extinct and only a few cytherellas, *D. stafeevi*, *C. ventriosum* and some other species persist but in small amounts. Further upsection, in the interval 27.5–29.0 m (samples 5–4) only a few specimens of the genus *Cytherella* (*C. ovata* (Roemer, 1841), *C. dilatata* Donze, 1964, *C. infrequens* Kuznetsova, 1961) and one valve of *Dolocythere rara* Mertens, 1956 were found. The uppermost part of the section (above ~30.5m, sample 3) is ostracod free.

Palynomorphs

All the samples studied contain a high amount of fragments from plant tissue and coal particles. The palynomorph assemblages are dominated by spores and pollen grains, while the dinocysts percentage is relatively low (at most 10 % of the total of palynomorphs; Supplementary Table S4). The total abundance of palynomorphs is highest in the middle part of the section (16.0–20.2 m, samples 15–10) and progressively decreases toward the top of the section.

On the basis of the changes in taxonomical composition and taxa proportions, two spore-pollen assemblages (PA) are distinguished (Fig. 6). PA1 corresponds to the lower part of the section (samples 23 and 19). It is dominated by pollen of the genus *Classopollis* (60 to 80 %), while fern and bryophyte spores are scarce.

The PA2 is defined in the interval from 10.7 m (sample 17) to the top of the studied succession. It is dominated by bisaccate pollens of gymnosperms and spores of Gleicheniaceae, while *Classopollis* become scarce. The level 16.5 m

(sample 13) is the unique episode of relatively increased *Classopollis* abundance (45 %) in this interval. Among the spores, species diversity and abundance of Schizaeaceae decreases, but several new taxa of Gleicheniaceae appear. The latter are represented by *Gleicheniidites*, *Clavifera*, *Ornamentifera granulata* and gradually tend to dominate the spore assemblage.

The dinocyst assemblages are characterized by low abundance but high species diversity (>80 taxa) (Supplementary Table S5). They are mostly badly preserved possibly as a result of unfavourable habitat and/or burial. Three dinocyst assemblages have been recognized.

The D1 assemblage is identified in the lowermost part of the section (0–7 m, samples 23, 19; Fig. 6). It is characterized by the occurrence of *Surculosphaeridium* sp. III *sensu* Davey, 1982, *Taleisphaera hydra* subsp. *elongata* (late Barremian of Germany, Heilmann-Clausen & Thomsen, 1995) (Supplementary Fig. S5, Table S5) and *Prolixosphaeridium parvispinum*, which has its FO in the late Barremian in both Boreal and Tethyan realms (Oosting et al. 2006). In the Zavodskaya Balka section, the D1 assemblage corresponds to the uppermost part of the *B. blowi* Zone and *H. ruka* Bed, and the greater part of the NC6A nannofossil Subzone.

The D2 assemblage was recognized in the interval 10.5–23.0 m (samples 17–8) and can be correlated to the dinocyst assemblage of the Bedoulian (Lower Aptian) of the Aptian stratotype sections in southern France (Davey & Verdier 1974). This D2 assemblage includes *Pseudoceratium polymorphum*, which has its FO in the lowermost part of the Aptian, and *Pseudoceratium securigerum* and *Palaeoperidinium cretaceum*, which show their FOs in the uppermost part of the Barremian (Heimhofer et al. 2007). The LO of *Muderongia* cf. *staurota sensu* Davey, Verdier, 1974 is found in the lower part of the early Aptian (Bedoulian) in the stratotype area. In the Zavodskaya Balka section, it occurs up to the level 10.8 m (sample 17). This assemblage ranges from the upper part of NC6A to the lower part of NC7C and the upper part of *H. excelsa* to the lower part of *H. trocoidea* Zones.

The D3 assemblage is found in the upper part of the section from 23.0 m (samples 6, 3 and 1) and is characterized by a decline of the majority of the species, which occurred in the lower part of the section. Only *Protoellipsodinium spinocristatum, Subtilisphaera perlucida*, *Pterospermella* sp., several acritarchs and green algae phytomata persist in this interval. The D3 assemblage correlates to the upper part of the NC7C Subzone and to the interval including the upper part of the *H. trocoidea* Zone and the *P. rohri* Zone.

Discussion and conclusion

The study of the upper Barremian–Aptian planktonic foraminifera, calcareous nannofossils, ostracods and palynomorphs of the Zavodskaya Balka showed similar trends in the distribution of these microfossil groups throughout the succession: the most abundant and diverse assemblages are found in the lower part of the section, all microfossils are progressively eliminated in the interval likely corresponding to OAE1a, recover part of their initial abundance above this event and decline again in the upper part of the section. Our results show the specificity of the occurrence of the late Barremian–Aptian microfossil markers of south-eastern Crimea and the correlation between the most important markers of different microfossil groups. The calcareous nannofossil assemblage of the Zavodskaya Balka section is typical for the Tethyan Barremian–Aptian interval, while PF, ostracods and dinocysts present some regional specificity. The succession of standard nannofossil zones and subzones was identified in the section, although subzonal boundaries within NC7 Zone are not certain due to scarcity or unreliable species definition of the markers (*M. hoschulzii* and *R. achlyostaurion*, respectively). The absence from our samples of several stratigraphically important PF species, such as *L. cabri, G. ferreolensis* and *G. algerianus*, caused a discontinuity in the recognition of several standard PF zones and thus prevented the direct correlation of the middle part of the section with the Tethyan PF zonations. The biohorizon characterized by the occurrence of *H. ruka*, recently established in the Lower Aptian of several sections from south-western Crimea, has been identified in the Zavodskaya Balka section in the upper half of the NC6A Subzone. The *H. excelsa* Zone, defined by the FO of the zonal marker, shows a larger stratigraphic range in the studied section than in the Tethyan area. It roughly corresponds to the upper part of NC6A and the greater part of NC6B and thus, covers the part of *L. cabri* Zone (Coccioni et al. 2007). The FOs of *H. trocoidea* and *P. rohri* are useful bioevents for subdivision of the late Aptian interval. The succession of ostracod bioevents in the Zavodskaya Balka section led to identification of three ostracod zones (*R. minima–L. variealveolat*a, *M. bicuspidata–R. minima* and *S. omnivaga*), recently established in south-western Crimea. The dinocyst distribution throughout the section showed the succession of three assemblages determined by the FOs of the marker species and dominance of different taxa.

The base of the Aptian in the section is based on the position of the magnetic reversal assumed to be the base of Chron M0. The upper Barremian part of the section corresponds to the lower half of the nannofossil NC6A Subzone, the greater part of the foraminiferal *B. blowi* Zone and the D1 dinocyst assemblage. The ostracod *L. variealveolata–R. minima* Zone approximately embraces the upper Barremian–lower Aptian part of the section.

The lower Aptian is characterized by the highest resolution in the stratigraphic subdivision based on nannofossil and ostracod study. Biostratigraphic subdivision of the series is made still more difficult and uncertain in the upper part of the section (upper upper Aptian) because of the scarcity of the microfossils.

One interesting result of this study is the recognition of an interval likely corresponding to the OAE1a, which has never been documented in the Aptian sedimentary record of the Crimea until now. It is preceded by a "nannoconid crisis" and

characterized by dramatically reduced productivity of microbiota. The specificity of this global event in the Crimea is the very low TOC content which makes its repercussion distinctive compared to many other world areas, where this event is featured by sediments rich in TOC (e.g., Jenkyns 1980; Arthur et al. 1990; Bralower et al. 1994; Föllmi 2012; Giorgioni 2015, a.o.). Our further study will be focused on the paleoecological reconstruction of the south-western Crimean basin in the late Barremian–Aptian with special emphasis on the OAE1a.

Acknowledgements: The authors are grateful to A.G. Manikin and M.I. Bagaeva, the Saratov State University and to I.M. Byakin for helping with the collection of samples for paleomagnetic study. We appreciate Prof. Michel Moullade, Dr. Milan Kohut and two anonymous reviewers a lot for their careful reading of the manuscript, many useful remarks and advice given to improve the paper. This study was made following the plans of the scientific research of the Geological Institute of RAS (for M. Karpuk, E. Brovina, E. Shcherbinina and E. Tesakova, project no. 0135-2018-0036). Field works were supported by RFBR projects nos. 16-35-00468 and 16-05-00363 (M. Karpuk and E. Brovina). Analytical data were derived with partial support of the RAS presidium program (for E. Shcherbinina and E. Shchepetova no. 0135-2018-0050).

References

Aguado R., Castro J.M., Company M. & De Gea G.A. 1999: Aptian bio-events—an integrated biostratigraphic analysis of the Almadich Formation, Inner Prebetic Domain, SE Spain. *Cretaceous Res.* 20, 663–683.

Arkadiev V.V. 2004: The first record of a late Tithonian ammonite in the Feodosiya section of Eastern Crimea. *Paleontol. J.* 38, 3, 265–267.

Arkadiev V.V. 2007: Zonation of the Berriasian sediments of the Mountain Crimea. *Vestnik of Saint Petersburg University, Earth sciences*, *ser. 7,* 2, 27–43 (in Russian).

Arkadiev V.V. 2011: New data on ammonoids of the genus *Paraulacosphinctes* from the upper Tithonian of the Mountainous Crimea. *Stratigraphy and Geological Correlation*, 19, 2, 238–242.

Arkadiev V.V., Grishchenko V.A., Guzhikov A.Yu., Manikin A.G., Savelieva Yu.N., Feodorova A.A. & Shurekova O.V. 2017: Ammonites and magnetostratigraphy of the Berriasian–Valanginian boundary deposits from eastern Crimea: *Geol. Carpath*., 68, 6, 505–516.

Arkadiev V., Guzhikov A., Baraboshkin E., Savelieva J., Feodorova A., Shurekova O., Platonov E. & Manikin A. 2018: Biostratigraphy and magnetostratigraphy of the upper Tithonian–Berriasian of the Crimean Mountains: *Cretaceous Res.* 87, 5–41.

Arthur M.A., Jenkyns H.C., Brumsack H.J. & Schlanger S.O. 1990: Stratigraphy, geochemistry, and paleoceanography of organic carbon–rich Cretaceous sequences. In: Ginsburg R.N. & Beaudoin B. (Eds.): Cretaceous Resources, Events and Rhythms: Background and Plans for Research, *NATO ASI Series*, C 304, 75–119.

Babinot J.-F., Damotte R., Donze P., Grosdidier E., Oertli, H.J. & Scarenzi-Carboni G. 1985: Cretace Inferieur, In Oertli H.J. (Ed.), Atlas des ostracodes de France (Paléozoïque-Actuel): *Bull. Centres Rech. Explor. Prod. Elf-Aquitaine*, 9, 163–210.

Bachmann M., Bassiouni M. A. A., & Kuss J. 2003: Timing of mid-Cretaceous carbonate platform depositional cycles, northern Sinai, Egypt. *Palaeogeogr. Palaeoclimatol. Palaeoecol.* 200, 131–162.

Bagaeva M.I. & Guzhikov A.Yu. 2014: Magnetic textures as indicators of formation of Tithonian-Berriasian rocks of the Mountain Crimea. *Izvestiya of Saratov University. New Series. Series: Earth Sciences* 14, 1, 41–47 (in Russian).

Baraboshkin E.Yu. 2016: Geological history of the Crimea. Precambrian–Early Cretaceous. In: Baraboshkin E.Yu. & Yaseneva E.V. (Eds.): Ecological and resource potential of the Crimea. *History of formation and prospects of development: VVM* 1, 38–84 (in Russian).

Baraboshkin E.Yu., Guzhikov A.Yu., Mutterlose J., Yampolskaya O.B., Pimenov M.V. & Gavrilov S.S. 2004: New data on stratigraphy of the Barremian-Aptian of the Mountain Crimea in accordance to finding of the analogue of the magnetochron M0 in the Verkhorechie section. *Vestnik of the Moscow State University, Geology series* 1, 10–20 (in Russian).

Bolii H. 1959: Planktonic foraminifera from the Cretaceous of Trinidad. *Bull. Amer. Paleontol.*, 257–277.

Bolli H. 1966: Zonation of cretaceous to pliocene marine sediments based on planktonic foraminifera. *Bol. Inform. Asoc. Venez. Geol., Miner., Petrol*. 9, 1, 3–32.

Bottini C., Erba E., Tiraboschi D., Jenkyns H.C., Schouten S. & Sinninghe Damsté J. S., 2015: Climate variability and ocean fertility during the Aptian Stage. *Climate of the Past*, 11, 383–402.

Bown P.R. & Young J.R. 1998: Techniques. In Bown P.R. (Ed.). Calcareous Nannofossil Btostratigraphy: *Kluwer Academic Press,* Dordrecht, 16–28.

Bown P.R., Rutledge D.C., Crux J.A. & Gallagher L.T., 1998: Lower Cretaceous. In: Bown P.R. (Ed.): Calcareous Nannofossil Biostratigraphy: *Kluwer Academic Press*, Dordrecht, 86–131.

Bralower T.J., Arthur M.A., Leckie R.M., Sliter W.V., Allard D.J. & Schlanger S.O. 1994: Timing and palaeoceanography of oceanic dysoxia/anoxia in the late Barremian to early Aptian (early Cretaceous). *Palaios* 9, 335–369.

Bralower T.J., Leckie R.M., Sliter W.V. & Therstein H. R. 1995. An intergrated Cretaceous microfossil biostratigraphy. In: Berggren W.A., Kent D.V. & Hardenbol, J. (Eds.), Geochronology, Time Scales and Global Stratigraphic Correlations: *SEPM Spec. Publ.* 54, 65–79.

Brovina E.A. 2017: Problems in stratigraphy of the upper Barremian – Aptian of the Cremia using planktonic foraminifera. *Stratigraphy and Geological Correlation*, 25, 5, 41–57 (in Russian).

Brovina E.A., Karpuk M.S., Shcherbinina E.A. & Tesakova E.M. 2017: Stratigraphy of r. Alma basin Aptian deposits based on new micropaleontological data. *Bulleten MOIP. Otd. Geologii*, 92, 6, 26–42 (in Russian).

Channell J.E.T., Erba E., Muttoni G. & Tremolada F. 2000: Early Cretaceous magnetic stratigraphy in the APTICORE drill core and adjacent outcrop at Cismon (Southern Alps, Italy), and correlation to the proposed Barremian–Aptian boundary stratotype. *GSA Bulletin* 112, 9, 1430–1443.

Coccioni R., Premoli Silva I., Marsili A. & Verga D. 2007: First radiation of Cretaceous planktonic foraminifera with radially elongate chambers at Angles (Southeastern France) and biostratigraphic implications. *Revue de micropaleontologie* 50, 215–224.

Coccioni R., Jovane L., Bancalà G., Bucci C., Fauth G., Frontalini F., Janikian L., Savian J., Paes De Almeida P., Mathias G.L. & Da Trindade R.I.F. 2012: Umbria-Marche Basin, Central Italy: A Reference Section for the Aptian-Albian Interval at Low Latitudes. *Scientific Drilling* 13, 42–46.

Coimbra J.C., Arai M. & Carreno A. L. 2002: Biostratigraphy of Lower Cretaceous microfossils from the Araripe basin, northeastern Brazil. *Geobios* 35, 687–698.

Damotte R., Babinot J.-F. & Colin J-P. 1981: Les Ostracodes du Cretace Moyen Europeen. *Cretaceous Res.* 2, 287–306.

Davey R. J. & Verdier J. P. 1974: Dinoflagellate cysts from the Aptian type sections at Gargas and La Bédoule, France. *Palaeontology* 17, 3, 623–653.

Debiche M.G. & Watson G.S. 1995: Confidence limits and bias correction for estimating angles between directions with applications to paleomagnetism. *Journal of Geophysical Research*, 100, B12, 24405–24430.

Erba E. 1994: Nannofossils and superplumes: The early Aptian "nannoconid crisis". *Paleoceanography* 9, 3, 483–501.

Erba E., & Tremolada F. 2004: Nannofossil carbonate fl uxes during the Early Cretaceous: Phytoplankton response to nutrifi cation episodes, atmospheric CO2 and anoxia. *Paleoceanography* 19, PA1008.

Erba E., Aguado R., Avram E., Baraboschkin E.J., Bergen J.A., Bralower T.J., Cecca F., Channell J.E.T., Coccioni R., Company M., Delanoy G., Erbacher J., Herbert T.D., Hoedemaeker P., Kakabadze M., Leereveld H., Lini A., Mikhailova I.A., Mutterlose J., Ogg J.G., Premoli Silva I., Rawson P.F., Von Salis K. & Weissert H. 1996: The Aptian stage: Bulletin de l'institut Royal des sciences naturelles de Belgique. *Proceedings "Second International Symposium on Cretaceous Stage Boundaries". Brussels 8 - 16 September 1995*, 31–43.

Erba E., Channell J.E.T., Claps M., Jones C., Larson R., Opdyke B., Premoli Silva I., Riva A., Salvini G., & Torricelli S. 1999: Integrated stratigraphy of the Cismon Apticore (southern Alps, Italy); a "reference section" for the Barremian-Aptian interval at low latitudes. *J. Foram. Res.* 29, 4, 371–391.

Flinn D., 1965: On the symmetry principle and the deformation ellipsoid. *Geol. Mag.* 102, 36–45.

Föllmi K.B. 2012: Early Cretaceous life, climate and anoxia. *Cretaceous Res.* 35, 230–257.

Gorbachik T.N. 1959: New foraminifera species from the lower Cretaceous deposits of the Crimea and SW Caucasus. *Paleontological Journal* 1, 78–83 (in Russian).

Gorbachik T.N. 1964: Variability and mircosturcture of the test wall of the Globigerinelloides algerianus Cushman et Dam. *Paleontological Journal* 4, 32–37 (in Russian).

Gorbachik T.N. 1969: Peculiarity of foraminifer distribution of in the Berriassian and Valanginian sediments of the Crimea. *Vestnik MSU, ser. 4, Geology* 4, 56–67 (in Russian).

Gorbachik T.N. 1986: Jurassic and Early Cretaceous planktonic foraminifera of the south of USSR. *Nauka*, Moskva, 1–239 (in Russian).

Gorbachik T.N. & Krechmar V. 1969: Stratigraphical subdivision of the Aptian and Albian sediments of the Crimea using planktonic foraminifera. *Vest. MSU, Ser. 4, Geology* 3, 46–56 (in Russian).

Giorgioni M., Keller C.E., Weissert H., Hochuli P.A. & Bernasconi S.M. 2015: Black shales — from coolhouse to greenhouse (early Aptian). *Cretaceous Res.* 56, 716–731.

Guzhikov A.Yu., Arkadiev V.V., Baraboshkin E.Yu., Bagaeva M.I., Piskunov V.K., Rudko S.V., Perminov V.A. & Manikin A.G. 2012: New sedimentological, bio-, and magnetostratigraphic data on the Jurassic–Cretaceous Boundary Interval of Eastern Crimea (Feodosiya). *Stratigraphy and Geological Correlation*, 20, 3, 261–294.

Guzhikov A., Bagayeva M. & Arkadiev V. 2014: Magnetostratigraphy of the Upper Berriasian "Zavodskaya Balka" section (East Crimea, Feodosiya). *Volumina Jurassica* XII, 1, 175–184.

Habermann A. & Mutterlose J. 1998. Early Aptian blackshales from NW Germany: calcareous nannofossils andtheir palaeoceanographic implications. *Neues Jahrb. Geol. Paläontol.* 212, 1–3, 379–400.

Heilmann-Clausen C. & Thomsen E. 1995: Barremian-Aptian dinoflagellates and calcareous nannofossils in the Ahlum 1 borehole and the Otto Gott clay pit, Sarstedt, Lower Saxony Basin, Germany. In Kemper E. (Ed.): The Barremian-Aptian Boundary. A Study of profiles from the Boreal Cretaceous. *Geologisches Jahrbuch Reihe A*, 141, 257–365.

Heimhofer U., Hochuli P.A., Burla S. & Weissert H. 2007: New records of Early Cretaceous angiosperm pollen from Portuguese coastal deposits: Implications for the timing of the early angiosperm radiation. *Review of Palaeobotany and Palynology*, 144, 39–76.

Jenkyns H.C. 1980: Cretaceous anoxic events: from continents to oceans: *J. Geol. Soc.* 137, 171–188.

Karpuk M.S. 2016a: New Protocytherines (Ostracods) from the Lower Cretaceous sequences of the Crimean Peninsula. *Revue de micropaléontologie* 59, 180–187.

Karpuk M.S. 2016b: Biostratigraphy of the upper Barremian–Aptian of the Mountain Crimea based on Ostracodes. In: Baraboshkin E.Yu. (Ed.): Proceedings of 8-th All-Russian Symposium on the Cretaceous system, Simferopol, 142–145 (in Russian).

Karpuk M.S. & Tesakova E.M. 2010: Lower Cretaceous ostracodes of the Verkhorechie section (SW Crimea). In: Baraboshkin E.Yu. (Ed.): Proceedings of 5-th All-Russian Symposium on the Cretaceous system, Ulianovsk, 188–191 (in Russian).

Karpuk M.S. & Tesakova E.M. 2013: New ostracods of the Family Cytheruridae G. Mueller from the Barremian-Albian of the Southwestern Crimea. *Paleontological Journal* (Moscow), 47, 6, 588–596.

Karpuk M.S. & Tesakova E.M. 2014: New ostracods of the families Loxoconchidae and Trachyleberididae from the Barremian-Albian of southwestern Crimea. *Paleontological Journal* 48, 2, 177–181.

Khramov A.N. (Ed.) 1982: Paleomagnetology: *Nedra*, St. Petersburg, 1–312 (in Russian).

Leckie R.M. 1987: Paleoecology of mid-Cretaceous planktonic foraminifera: A comparison of open ocean and Epicontinental Sea assemblages. *Micropaleontology* 33, 2, 164–176.

Lott G.K., Ball K.C. & Wilkinson I.P. 1985: Mid-Cretaceous stratigraphy of a cored borehole in the western part of the Central North Sea Basin. *Proceedings of the Yorkshire Geological Society* 45, 4, 235–248.

Lott G.K., Fletcher B. N. & Wilkinson I.P. 1986: The stratigraphy of the Lower Cretaceous Speeton Clay Formation in a cored borehole off the coast of north-east England. *Proceedings of the Yorkshire Geological Society* 46, 1, 39–56.

Luciani V., Cobianchi M. & Lupi C. 2006: Regional record of a global oceanic anoxic event: OAE1a on the Apulia Platform margin, Gargano Promontory, southern Italy. *Cretaceous Res.* 27, 754–772.

Moullade M. 1966. Etude stratigraphique et micropaléontologique du créetacé inférieur de la "fosse vocontienne". Stratigraphy. *Université de Lyon*, 1–369.

Moullade M. 1974: Zones de foraminiferes du cretace inferieur mesogeen. *Comptes Rendus Hebdomadaires des Séances de l'Académie des Sciences de Paris* D278, 1813–1816.

Moullade M., Tronchetti G., Busnardo R. & Masse J.-P. 1998a. Description lithologique des coupes types du stratotype historique de l'Aptien inférieur dans la région de Cassis-La Bédoule (SE France). *Géologie Méditerranéenne* 25, 15–29.

Moullade M., Masse J.-P., Tronchetti G., Kuhnt W., Ropolo P., Bergen J.A., Masure E. & Renard M. 1998b. Le stratotype historique de l'Aptien inférieur dans la région de Cassis-La Bédoule (SE France): Synthèse stratigraphique. *Géologie Méditerranéenne* 25, 289–298.

Moullade M., Tronchetti G. & Bellier J.-P. 2005: The Gargasian (Middle Aptian) strata from Cassis-La Bédoule (Lower Aptian historical stratotype, SE France): Planktonic and benthic foraminiferal assemblages and biostratigraphy. *Carnets de Géologie*, Article 2005/02, 1–20.

Moullade M., Granier B. & Tronchetti G. 2011: The Aptian Stage: Back to fundamentals. *Episodes* 34, 3, 148–156.

Moullade M., Tronchetti G., Granier B., Bornemann A., Kuhnt W. & Lorenzen J. 2015: High-resolution integrated stratigraphy of the OAE1a and enclosing strata from core drillings in the Bedoulian stratotype (Roquefort-La Bedoule, SE France). *Cretaceous Res.* 56, 119–140.

Neale J.W. 1978: A stratigraphycal index of British Ostracoda. In: Bate R. & Robinson E. (Eds.): *Geol. J.* Spec. Iss. 8, 325–384.

Nemirovskaya T.N. 1972: About the Barremian and Aptian ostracods of the South-Western Crimea. In: Questions about the geology of the sedimentary basins of the Ukraine. Kiev, 15–20 (in Russian).

Ogg J.G. & Hinnov L.A. 2012: Cretaceous. In: Gradstein F.M., Ogg J.G., Schmitz M.D. & Ogg G.M. (Eds.): Geological Time Scale. *Elsevier*, 793–853.

Ogg J.G., Ogg G.M. & Gradstein F.M. 2016: A Concise Geologic Time Scale, *Elsevier*, Amsterdam, 1–230.

Oosting A.M., Leereveld H., Dickens G.R., Henderson R.A. & Brinkhuis H. 2006. Correlation of Barremian-Aptian (mid-Cretaceous) dinoflagellate cyst assemblages between the Tethyan and Austral realms. *Cretaceous Res.* 27, 6, 792–813.

Opdyke N.D. & Channell J.E.T. 1996: Magnetic Stratigraphy. *Academic press*. N.Y., 1–344.

Patruno S., Triantaphyllou M.V., Erba E., Dimiza M.D., Bottini C. & Kaminski M.A. 2015. The Barremian and Aptian stepwise development of the 'Oceanic Anoxic Event 1a' (OAE 1a) crisis: Integrated benthic and planktic high-resolution palaeoecology along the Gorgo a Cerbara stratotype section (Umbria–Marche Basin, Italy). *Palaeogeogr. Palaeoclimatol. Palaeoecol.* 424, 147–182.

Premoli Silva I., Caron M., Leckie R.M., Petrizzo M.R., Soldan D. & Verga D. 2009. Paraticinella n. gen. and taxonomic revision of Ticinella bejaouaensis Sigal, 1966. *The Journal of Foraminiferal Research* 39, 2, 126–137.

Reboulet S., Szives O., Aguirre-Urreta B., Barragán R., Company M., Idakieva V., Ivanov M., Kakabadze M.V., Moreno-Bedmar J.A, Sandoval J., Baraboshkin E.J., Çaglar M.K., Fozy I., González-Arreola C., Kenjo S., Lukeneder A., Raisossadat S.N., Rawson P.F. & Tavera J.M. 2014: Report on the 5th International Meeting of the IUGS Lower Cretaceous Ammonite Working Group, the Kilian Group (Ankara, Turkey, 31st August 2013). *Cretaceous Res.* 50, 126–137.

Risch H. 1971: Stratigraphie der höheren Unterkreide der bayerischen Kalkalpen mit Hilfe von Mikrofossilien. *Palaeontographica Abteilung* A138, 1–80.

Roth P.H. 1978: Cretaceous nannoplankton biostratigraphy and oceanography of the northwestern Atlantic Ocean. In: Benson W.E., Sheridan R.E. et al. (Eds.): *Init. Repts. DSDP* 44, Washington (U.S. Govt. Printing Office), 731–759.

Salman G.B. & Dobrovolskaya T.I. 1968: The Valanginian–Barremian conglomerates of the eastern Crimea. *Proceedings of the Academy of Sciences of USSR*, 133, 6, 1432–1434 (in Russian).

Savian J., Trindade R., Janikian L., Jovane L., Paes de Almeida P., Coccioni R., Frontalini F., Sideri M., Figueiredo M., Tedeschi L.R. & Jenkins J. 2016: The Barremian-Aptian boundary in the Poggio le Guaine core (central Italy): Evidence for magnetic polarity Chron M0r and oceanic anoxic event 1a. *The Geological Society of America Special Paper* 524, 57–78.

Shcherbinina E.A. & Loginov M.A. 2012: Lower Cretaceous nannofossilstratigraphy of the Sw Crimea. In: Vishnevskaya V.S., Goreva N.V. & Filimonova T.V. (Eds.): Proceedings of XVth Allrussian micropaleontological symposium, Gelendzhik, 324–327 (in Russian).

Shcherbinina E., Gavrilov Yu., Iakovleva A., Pokrovsky B., Golovanova O. & Aleksandrova G., 2016. Environmental dynamics during the Paleocene–Eocene thermal maximum (PETM) in the northeastern Peri-Tethys revealed by high-resolution micropalaeontological and geochemical studies of a Caucasian key section. *Palaeogeogr. Palaeoclimatol. Palaeoecol.* 456, 60–81.

Shumenko S.I. 1974: Lower Cretaceous calcareous nannofossils of the Crimea. *Bulletin of the High Scools, Geology and Exploration Series* N9, 52–60 (in Russian).

Shurekova O.V. 2016: Stratigraphical scale based on dinocysts for lower Cretaceous of the Crimea. In: Tolmacheva T.Yu. (Ed.) :Proceedings of the workshop: Stratigraphical scale and methodical problems in regional Russian stratigraphical scales development, 188–190.

Sigal J. 1977: Essai de zonation du cretace mediterranean a l'aide des foraminiferes planctoniques. *Géologie méditerranéenne* 4, 49–108.

Sissingh W. 1977: Biostratigraphy of Cretaceous calcareous nannoplankton. *Geol. Mijnbouwn*, 56, 37–50.

Sohn I.G. 1961: Techniques for preparation and study of fossil ostracods. In: Treatise on Invertebrate Paleontology. Part Q, Arthropoda 3, Crustacea, Ostracoda, 64–70.

Szives O., Fodor L., Fogarasi A. & Kövér Sz. 2018: Integrated calcareous nannofossil and ammonite data from the upper Barremian – lower Albian of the northeastern Transdanubian Range (central Hungary): Stratigraphical implications and consequences for dating tectonic events. Cretaceous Research 91, 229–250.

Van Der Voo R. 1993: Palaeomagnetism of the Atlantic, Tethys, and Iapetus oceans, Cambridge. *Cambridge University Press*, 1–412 .

Vishnevsky A.V. & Menaylenko P.A. 1963: Coccolithoforids of the lower Cretaceous (Aptian) clays of the Bakhchisaray area. *Bulletin of the High Scools, Geology and Exploration Series* 11, 47–53 (in Russian).

Viviers M.C., Koutsoukos E.A.M., da Silva-Telles A.C. Jr. & Bengtson P. 2000: Stratigraphy and biogeographic affinities of the late Aptian–Campanian ostracods of the Potiguar and Sergipe basins in northeastern Brazil. *Cretaceous Res.* 21, 407–455.

Wilkinson I.P. 1988: Ostracoda across the Albian/Cenomanian Boundary in Cambredgeshire and Western Suffolk, Eastern England. Evolutionary Biology of Ostracoda its fundamentals and applications. In: Hanai T., Ikeya N. & Ishizaki K. (Eds.): *Developments in Palaeontology and Stratigraphy*, 11, 1229–1244.

Wilkinson I.P. 2008: The effect of environmental change on early Aptian ostracods faunas in the Wessex Basin, southern England. *Revue de micropaleontology* 51, 259–272.

Wilkinson I.P. & Morter A.A. 1981: The biostratigraphical zonation of the East Anglian Gault by Ostracoda. In: Neale J.W. & Brasier M.D. (Eds.): Microfossils from Recent and Fossil Sherf-Seas. *Ellis Horwood, Ltd*., Chichester. 163–176.

Woods M.A., Wilkinson I. P., Dunn J. & Ridingl J. B. 2001: The biostratigraphy of the Gault and Upper Greensand formations (Middle and Upper Albian) in the BGS Selborne boreholes, Hampshire. In: BGS Selborne boreholes, Hampshire. *Proceedings of the Geologists' Association* 112, 211–222.

Yampolskaya O.B., Baraboshkin E.Yu., Guzhikov A.Yu., Pimenov M.V. & Nikulshin A.S. 2006: Paleomagnetic column of the Lower Cretaceous of the South-Western Crimea. *Vestnik of the Moscow State University, Geology series* 1, 3–15.

Supplement

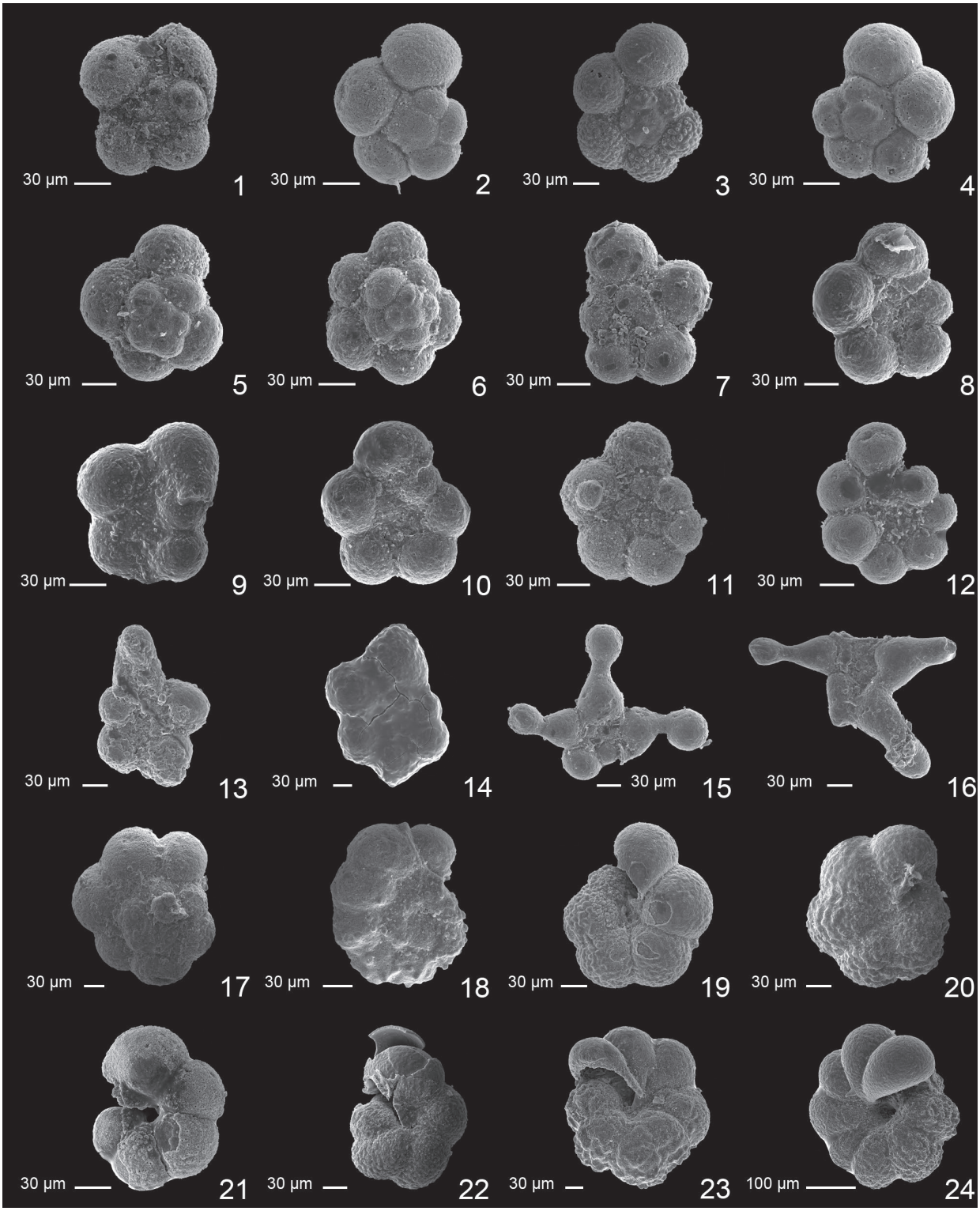

Fig. S1. SEM images of planktonic foraminifera from Zavodskaya Balka section: **1** — *Blowiella blowi* Bolli, 1959, sample 18; **2–4** —*Hedbergella infracretacea* (Glaessner, 1937): 2 — sample 14, 3 — sample 5, 4 — sample 19; **5** — *Hedbergella ruka* (Banner, Copestake and White, 1993), sample 17; **6** — *Hedbergella excelsa* Longoria, 1974, sample 17; **7–8** — *Hedbergella aptiana* Bartenstein, 1965, sample 16; **9** — *Hedbergella sigali* Moullade, 1966, sample 16; **10** — *Hedbergella similis* Longoria 1974, sample 16; **11** — *Hedbergella primare* (Kretchmar and Gorbachik, in Gorbachik, 1986), sample 14; **12** — *Hedbergella luterbacheri* Longoria, 1974, sample 15; **13** — *Hedbergella roblesae* (Obregon, 1959), sample 1504; **14** — *Hedbergella kuhryi* Longoria, 1974, sample 1503; **15–16** — *Leupoldina reicheli* (Bolli, 1957), sample 1504; **17** — *Hedbergella trocoidea* (Gandolfi, 1942), sample 09; **18** — *Planomalina cheniourensis* (Sigal, 1952), sample 08; **19–21** — *Paraticinella rohri* Bolli, 1959, juvenile tests: 19, 21 — sample 4, 20 — sample 5; **22–24** — *Paraticinella rohri* Bolli, 1959, adult tests, sample 4.

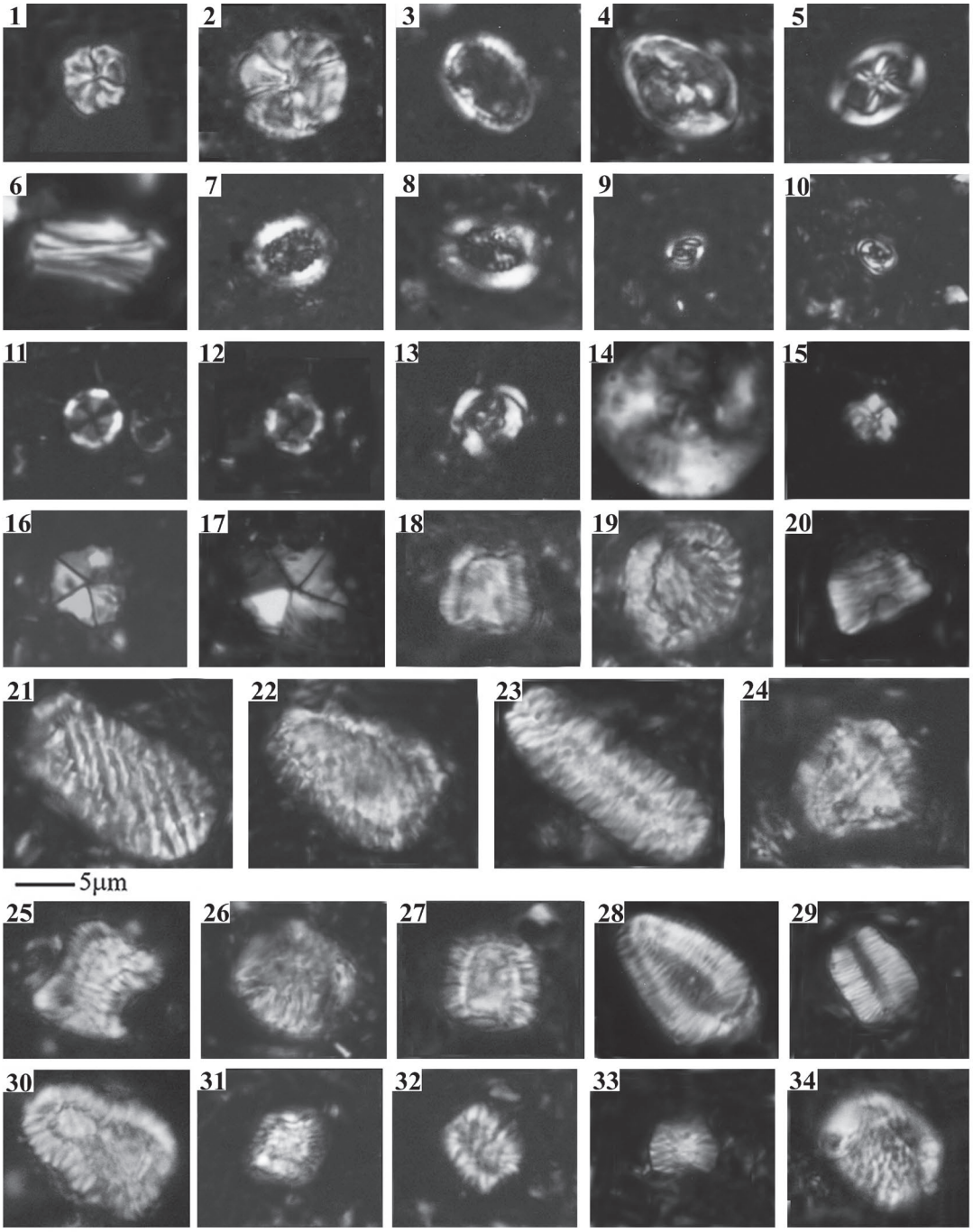

Fig. S2. Microphotographs of nannofossils from Zavodskaya Balka section. All images are made under cross-polarization of light microscope. **1** — *Assipetra terebrodentarius terebrodentarius* Applegate et al., 2007, sample 20; **2** — *A. terebrodentarius youngii* Tremolada et Erba, 2002, sample 17; **3** — *Axopodorhabdus dietzmannii* (Reinhardt, 1965) Wind & Wise, 1983, sample 19; **4** — *Calcicalathina oblongata* (Worsley, 1971) Thierstein, 1971, sample 18; **5** — *Chiastozygus litterarius* (Górka, 1957) Manivit, 1971, sample 5; **6** — *Conusphaera rothii* (Thierstein, 1971) Jakubowski, 1986, sample 17; **7** — *Cretarhabdus conicus* Bramlette et Martini, 1964, sample 7; **8** — *C. striatus* (Stradner, 1963) Black, 1973, sample 8; **9** — *Crucibiscutum bosunensis* Jeremiah, 2001, sample 8; **10** — *Eiffellithus hancockii* Burnett, 1997, sample 10; **11** — *Eprolithus floralis* (Stradner, 1962) Stover, 1966, sample 1503; **12** — *Farhania varolii* (Jakubowski, 1986) Varol, 1992, sample 8; **13** — *Flabellites oblongus* (Bukry, 1969) Crux in Crux et al., 1982, sample 20; **14** — *Haquis cyrcumradiatus* (Stover, 1966), sample 15; **15** — *Hayesites irregularis* (Thierstein in Roth & Thierstein, 1972) Applegate et al. in Covington & Wise, 1987, sample 16; **16** — *Micrantolithus hoschulzii* (Reinhardt, 1966) Thierstein, 1971, sample 23; **17** — *M. obtusus* Stradner, 1963, sample 20; **18** — *Nannoconus bucheri* Brönnimann, 1955, sample 23; **19** — *N. circularis* Deres et Achéritéguy, 1980, sample 23; **20** — *N. inornatus* Rutledge et Bown, 1996, sample 23; **21, 22** — *N. kamptneri* Brönnimann, 1955, sample 23; **23** — *N. elongatus* Brönnimann, 1955, sample 18; **24** — *N. vocontiensis* Deres et Achéritéguy, 1980, sample 1504; **25** — N. donnatensis Deres et Acherit, sample 1504; **26** — *N. globulus* Brönnimann, 1955, sample 17; **27** — *N. quadriangulus* Deflandre et Deflandre-Rigaud, 1962, sample 1504; **28, 29** — *N. steinmannii* Kamptner, 1931: 28 — sample 18, 29 — sample 19; **30** — *N. wassallii* Brönnimann, 1955, sample 23; **31** — *N. truitti* truitti Brönnimann, 1955,, sample 1504; **32** — *N. truitti* frequence Deres et Achéritéguy, 1980, sample 1504; **33** — *N. truitti* rectangularis Deres et Achéritéguy, 1980, sample 23; **34** — *Nannoconus* sp., sample 17.

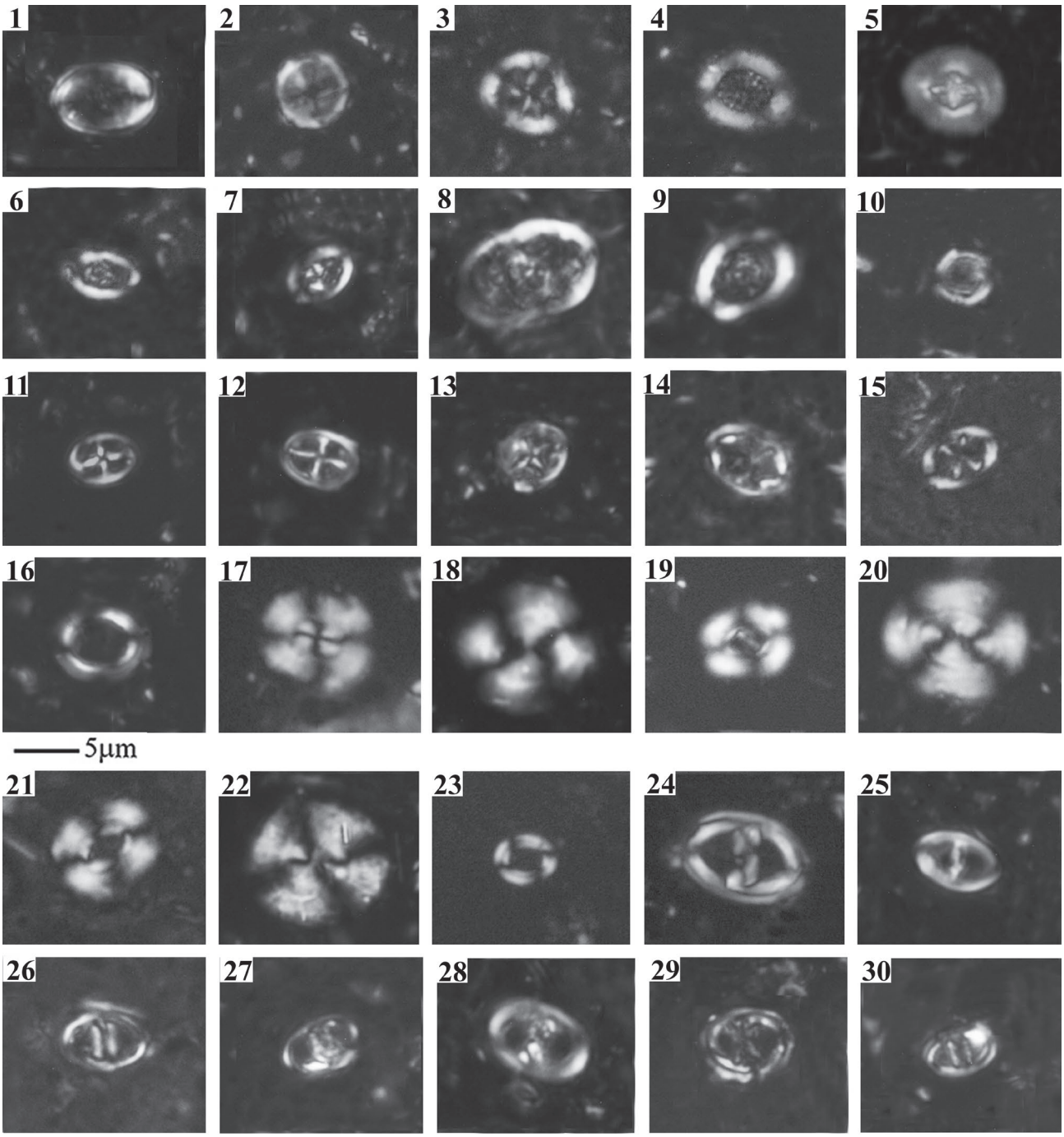

Fig. S3. Microphotographs of nannofossils from Zavodskaya Balka section. All images are made under cross-polarization of light microscope. **1** — *Percivalia fenestrata* (Worsley, 1971) Wise, 1983, sample 23; **2** — *Radiolithus planus* Stover, 1966, sample 8; **3** — *Retecapsa angustiforata* Black, 1971, sample 20; **4** — *R. crenulata* (Bramlette & Martini, 1964) Grün in Grün and Allemann, 1975, sample 10; **5** — *Pickelhaube*? sp., sample 8; **6** — *Rhagodiscus* cf. *achlyostaurion* (Hill, 1976) Doeven, 1983, sample 20; **7** — *R. achlyostaurion* (Hill, 1976) Doeven, 1983, sample 9; **8** — *R. amplus* Bown, 2005, sample 18; **9** — *R. asper* (Stradner, 1963) Reinhardt, 1967, sample 22; **10** — *Rotelapillus laffitei* Caratini, 1963, sample 21; **11** — *Staurolithites crux* (Deflandre et Fert, 1954) Caratini, 1963, sample 5; **12** — *S. mutterlosei* Crux, 1989, sample 18; **13** — S. siesseri Bown in Kennedy et al., 2000, sample 1503; **14** — *Stoverius acutus* (Thierstein in Roth & Thierstein, 1972) Young & Bown 2014, sample 10; **15** — *Tegumentum stradneri* Thierstein in Roth & Thierstein, 1972, sample 8; **16** — *Tubodiscus burnettiae* Bown in Kennedy et al., 2000, sample 21; **17** — *Watznaueria barnesiae* (Black in Black and Barnes, 1959) Perch-Nielsen, 1968, sample 9; **18** — *W. biporta* Bukry, 1969, sample 11; **19** — *W. britannica* (Stradner, 1963) Reinhardt, 1964, sample 1504; **20** — *W. cynthiae* Worsley, 1971, sample 23; **21** — *W. fossacincta* (Black, 1971) Bown in Bown & Cooper, 1989, sample 8; **22** — *W. manivitae* Bukry, 1973, sample 9; **23** — *W. ovata* Bukry, 1969, sample 8; **24** — *Zeugrhabdotus embergeri* (Noël, 1959) Perch-Nielsen, 1984, sample 8; **25** — *Z. erectus* (Deflandre in Deflandre & Fert, 1954) Reinhardt, 1965, sample 19; **26** — *Z. diplogrammus* (Deflandre in Deflandre & Fert, 1954) Burnett in Gale et al., 1996, sample 7; **27** — *Z. howei* Bown in Kennedy et al., 2000, sample 21; **28** — *Z. noeliae* Rood et al., 1971, sample 10; **29** — *Z. streetiae* Bown in Kennedy et al., 2000, sample 9; **30** — *Z. xenotus* (Stover, 1966) Burnett in Gale et al., 1996, sample 22.

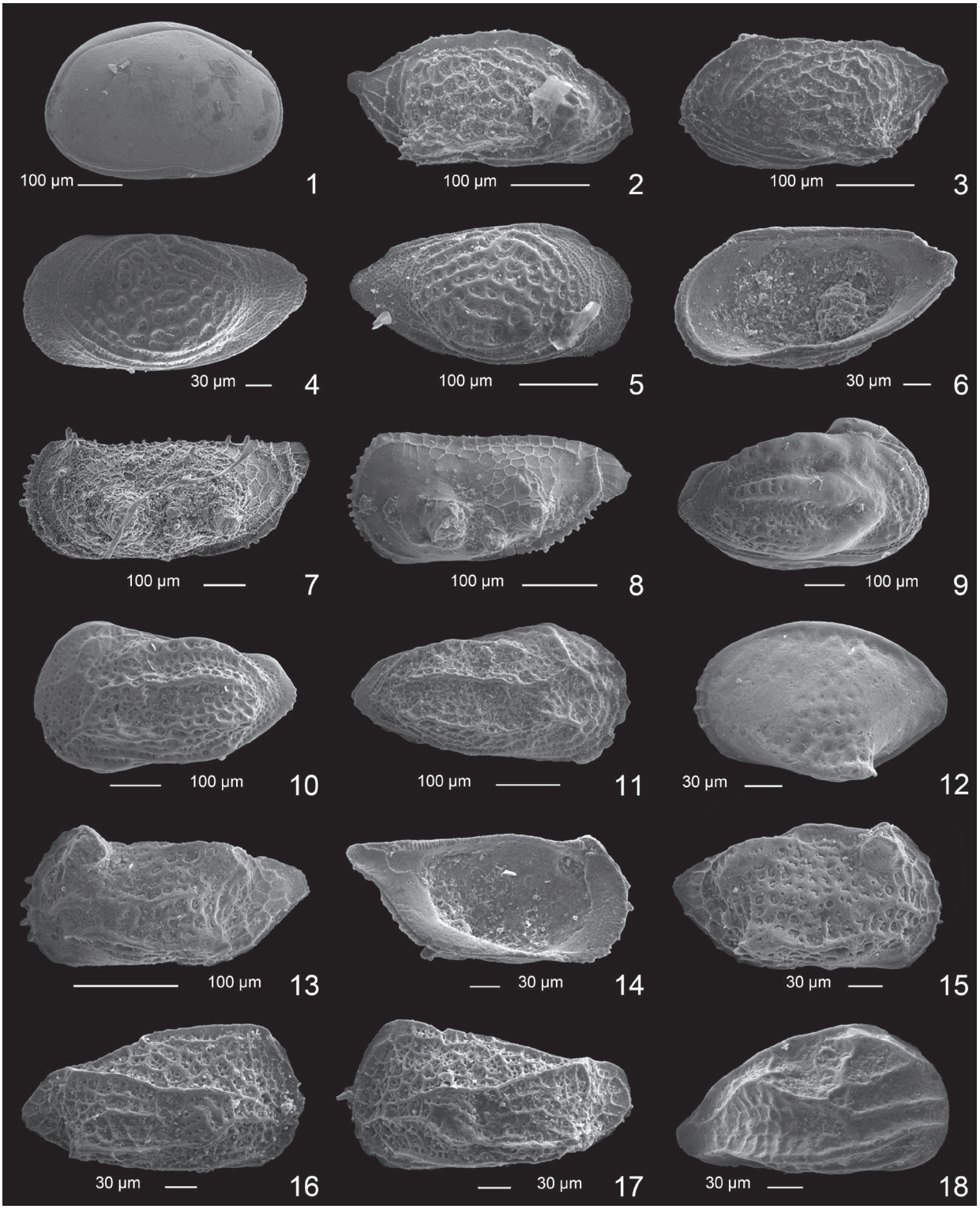

Fig. S4. SEM images of ostracodes from Zavodskaya Balka section: **1** — *Robsoniella minima* Kuznetsova, 1961. Adult carapace, right external view, sample 17; **2–3** — *Cytheropteron* sp. 3: 2 — Exterior view of adult RV, sample 15, 3 — Exterior view of adult LV, sample 15; **4–6** — *Loxoella variealveolata* Kuznetsova, 1956: 4 — Exterior view of adult LV, sample 16, 5 — Exterior view of adult RV, sample 15, 6 — Interior view of adult RV, sample 15; **7–8** — *Monoceratina bicuspidata* (Gründel, 1964), 1964: 7 — Exterior view of adult LV, sample 1504, 8 — Exterior view of juvenile LV, sample 8; 9 — *Protocythere* sp. Adult carapace, right external view, sample 9; **10–11** — *Saxocythere omnivaga* (Lyubimova, 1965). 10 — Exterior view of adult LV, sample 9, 11 — Exterior view of adult RV, sample 9; **12** — *Cytheropteron latebrosum* Kuznetsova, 1962. Exterior view of adult LV, sample 9; **13–14** — *Eucytherura mirifica* (Kuznetsova, 1961): 13 — Exterior view of adult LV, sample 17, 14 — Interior view of adult LV, sample 17; **15** — *Eucytherura* sp. 1. Exterior view of adult RV, sample 15; **16–17** — *Dorsocythere stafeevi* Karpuk et Tesakova, 2013: 16 — Exterior view of adult RV, sample 7, 17 — Exterior view of adult LV, sample 7; **18** — *Pleurocythere costaflexuosa* (Kuznetsova, 1961), 1957. Exterior view of adult RV, sample 18.

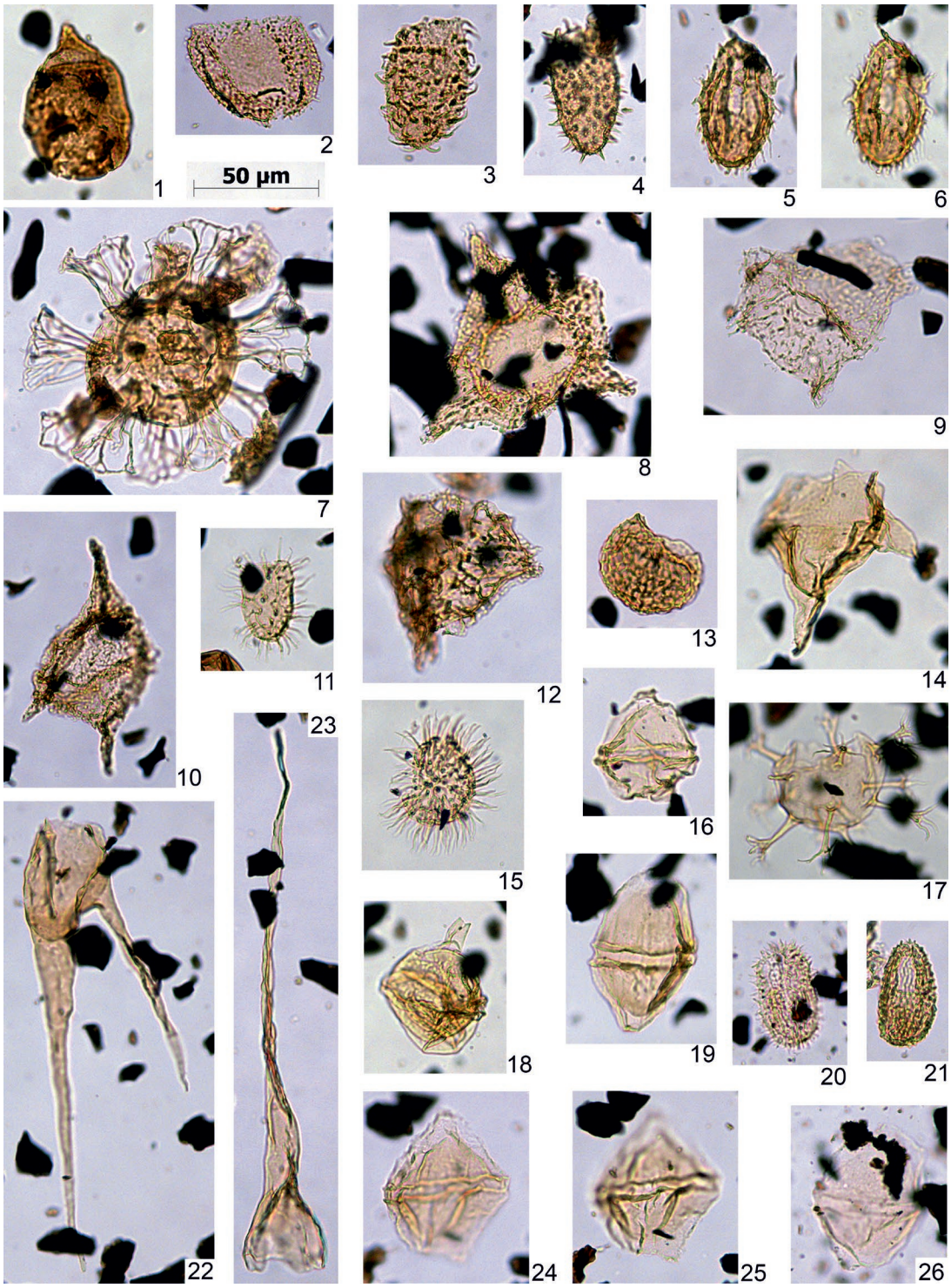

Fig. S5. Microphotographs of dinocysts from Zavodskaya Balka section: **1** — *Pareodinia* sp., sample 23; **2** — cf. *Circulodinium deflandrei* Alberti, 1961, sample 23; **3–4** — *Prolixosphaeridium parvispinum* (Deflandre, 1937) Davey et al., 1966, sample 23; **5–6** — *Taleisphaera hydra* subsp. *elongata* Heilmann-Clausen, 1995, sample 19; **7** — *Stiphrosphaeridium anthophorum* (Cookson et Eisenack, 1958) Davey, 1982, sample 17; **8** — *Pseudoceratium securigerum* (Davey et Verdier, 1974) Bint, 1986, sample 17; **9** — cf. *Pseudoceratium retusum* Brideaux, 1977, sample 12; **10** — *Pseudoceratium pelliferum* Gocht, 1957, sample 17; **11**— *Tanyosphaeridium* sp., sample 23; **12** — *Pseudoceratium polymorphum* (Eisenack, 1958) Bint, 1986, sample 12; **13** — *Cassiculosphaeridia sarstedtensis* Below, 1982, sample 12; **14** — *Muderongia* cf. *staurota* sensu Davey et Verdier, 1974, sample 19; **15** — *Cleistosphaeridium* sp., sample 15; **16** — *Subtilisphaera perlucida* (Alberti, 1959) Jain et Millepied, 1973, sample 8; **17** — *Oligosphaeridium*? *asterigerum* (Gocht, 1959) Davey et Williams, 1969, sample 19; **18** — *Dingodinium*? *albertii* Sarjeant, 1966, sample 23; **19** — *Subtilisphaera perlucida* (Alberti, 1959) Jain et Millepied, 1973, sample 8; **20** — *Protoellipsodinium spinocristatum* Davey et Verdier, 1971, sample 6; **21** — *Protoellipsodinium spinocristatum* Davey et Verdier, 1971, sample 12; **22–23** — *Odontochitina operculata* (Wetzel, 1933) Deflandre et Cookson, 1955, 22 — sample 15, 23 — sample 12; **24–25** — *Subtilisphaera perlucida* (Alberti, 1959) Jain et Millepied, 1973, sample 3; **26** — *Subtilisphaera perlucida* (Alberti, 1959) Jain et Millepied, 1973, sample 6.

Table S1: The PF range chart of Zavodskaya Balka section. Symbols: a — abundant (20 specimens in the picked up material, p.m.), c — common (10–20 specimens in the p.m.), r — rare (3–10 specimens in the p.m.), f — few (1–2 specimens in the p.m.).

Substages	Foraminifera zones	Sample nos. / Species	*Hedbergella infracretacea*	*Blowiella blowi*	*Hedbergella ruka*	*Hedbergella excelsa*	*Hedbergella sigali*	*Hedbergella aptiana*	*Hedbergella similis*	*Hedbergella primare*	*Hedbergella luterbacheri*	*Hedbergella roblesae*	*Hedbergella kuhryi*	*Leupoldina reicheli*	*Hedbergella trocoidea*	*Planomalina cheniourensis*	*Paraticinella rohri*
Upper Aptian	*P. rohri*	1	f														
		2	f												f		
		3	f														f
		4	f				f			f							r
		5	f														r
		6	a														r
	H. trocoidea	7	a														
		8	a												r	f	
		9	a												r		
Lower Aptian	*	10	a														
		11	a					r	r	r							
		1505	c				r	r	r	r	f	f					
		1504	c				r	r	r	r	r	f	f	r			
		1503	r				c	c	r	r	r	f	f	r			
	H. excelsa	13	f			f		f									
		1502	r			f											
		1501	c			f											
		14	r							f							
		15	c			r											
		16	r			r	f	f	f								
		17	f		r	r											
	**	18	f	f	r												
U. Barremian	*B. blowi*	19	f	f													
		20	f	f													
		21	f	f													
		22	f	f													
		23	f	f													

* - *H. luterbacheri* ** - *H. ruka* Bed

Table S2: The nannofossil range chart of Zavodskaya Balka section. Symbols: a — abundant (5 specimens per field of view, f.v.), c — common (1–4 specimens per f.v.), r — rare (several specimens per the row of the smear-slide), f — few (several specimens in the smear-slide).

Substages	Nannofossils zones	Sample nos. / Nannofossils species	1	2	3	4	5	6	7	8	9	10	11	1505	1504	1503	13	1502	1501	14	15	16	17	18	19	20	21	22	23
U. Barremian																													
Lower Aptian	NC6A	*Assipetra terebrodentarius*	f		f		f	f		f		f	f		f	f	f			f	f	f	f	f	f	f	f	f	f
		Flabellites oblongus	f				f	f		r	r	r	f		f	f	f			f	r	f	f	r	f	f	f	f	f
		Hayesites irregularis	f				f	f					f		f	f						f	f		f	r	f	f	f
		Litharaphidites carniolensis	f				f	f	f	f	f	f	f		f							f	f	r	f	r	f	f	f
		Rotelapillus laffittei	f	r			f	c	c	f	f	f	f		f	a						f	f	f	f	f	f	f	f
		Watznaueria barnesae/fossacincta			f	f	c	c	c	c	a	c	c		a	a	r			c	a	f	c	f	a	a	c	f	f
		Reinhardtites anthophorus																											
		Reinhardtites levis																											
		Reinhardtites mirabilis																											
		Retecapsa crenulata						f		c	f	c	f	f	f	r	f			f	f	f	f	f	c	r	f	f	f
		Rhagodiscus asper					f	f	f	c	f	c	f	f	r	r	f			f	f	c	r	c	f	c	f	f	f
		Zeugrhabdotus diplogrammus					f	f	f	f	f	f	f	f	f					f	f	f	f	f	f	f	f	f	f
		Zeugrhabdotus embergeri					f			f	f	f	f	f	f					f	f	f	f	f	f	f	f	f	f
		Zeugrhabdotus howei						f			f	f																	
		Retecapsa angustiphorata							f							f				f	f		f	f	f	f	f	f	f
		Zeugrhabdotus erectus								f			f	f	f	f					f		f	f	f	c	f	f	f
		Nannoconus truitii										f	f		c	f					f	f	f	r	f	f	f	f	f
		Nannoconus circularis													f	f					f	f	f		f	f	f	f	f
		Nannoconus steinmannii													f	f								r	f	f	f	f	f
		Nannoconus wassalii													f	f													
		Nannoconus bucheri													c									f					
		Micrantholithus hoschulzii													f										f	f	f	f	f
		Micrantholithus obtusus																		f	f	f	f	f	f	f	f	r	f
		Percivalia fenestrata																			f	f		f	f	f	f	f	f
		Conusphaera rothii																					f	f	f	f	f	f	f
		Nannoconus imbricatus																						f	f	f	r	f	f
		Nannoconus bonetii																											f
		Nannoconus kamptneri																											f
		Watznaueria britannica	f				f			f			f		f		f			f					f		f	f	
		Haquis circumradiatus					f				f				f	f												f	f
		Zeugrhabdotus xenotus																							f	f	f	f	f
		Axopodorhabdus dietzmannii																											
		Tubodiscus burnettiae	f									f	f	f	f	f				f	f		f	f	f	f	f		
		Rhagodiscus amplus					f				f	f	f	r	f	f					f	f	f	f	f	f	f		
		Watznaueria manivitae						f	f		f	f	f									f	f	f	f	f	f		
		Assipetra terebrodentarius youngii								f			f			f	f			f				f	f	f			
		Nannoconus voconiensis													f														
		Chiastozygus litterarius					f			f	f														f				
		Manivitella pemmatoidea						f	f			f			f	f	f			f				f	f				
		Cretarhabdus striatus								f	f				f	f									f	f			
		Nannoconus elongatus													f	f										f			
		Staurolithites multerlosii												f	f	f	f			f	f				f	f			
		Zygrhabdotus noeliae																							f	f			
		Biscutum constans								f		f		f	f	f									f	f			
		Nannoconus globulus																								f			
		Cretarhabdus conicus				f	f	f	f	f	f	f	f	f	f						f	f	f						
		Crucibiscutum bosunensis				f	f														f	f	f						
		Tegumentum stradneri					f	f		f	f	f	f	f							f	f	f						
		Grantarhabdus coronadventis							f		f	f	f									f							
		Staurolithites sciesseri					f					f	f																
		Repagulum parvidentatum						f									f			f	f								
		Eprolithus floralis								f	f	f	f			f													
		Farhania varolii									f	f				f													
		Nannoconus donatensis													f	f													
		Nannoconus quadricanalis													f														
		Eiffellithus hankockii	f	f								f	f	f															
		Watznaueria biporta	f	f									f	f															
		Stoverius acutus												f															
		Radiolithus planus						f	f	f	f	f																	
		Zeugrhabdotus streetiae						f	f		f	f																	
		Rhagodiscus achlyostaurion	f				f	f	f	f	f																		
		Calcicalathina erbae				f																							
		Pickelhaube furtiva					f			f																			

Table S3: The ostracod range chart of Zavodskaya Balka section. Numbers are the abundance of specimens found in the sample.

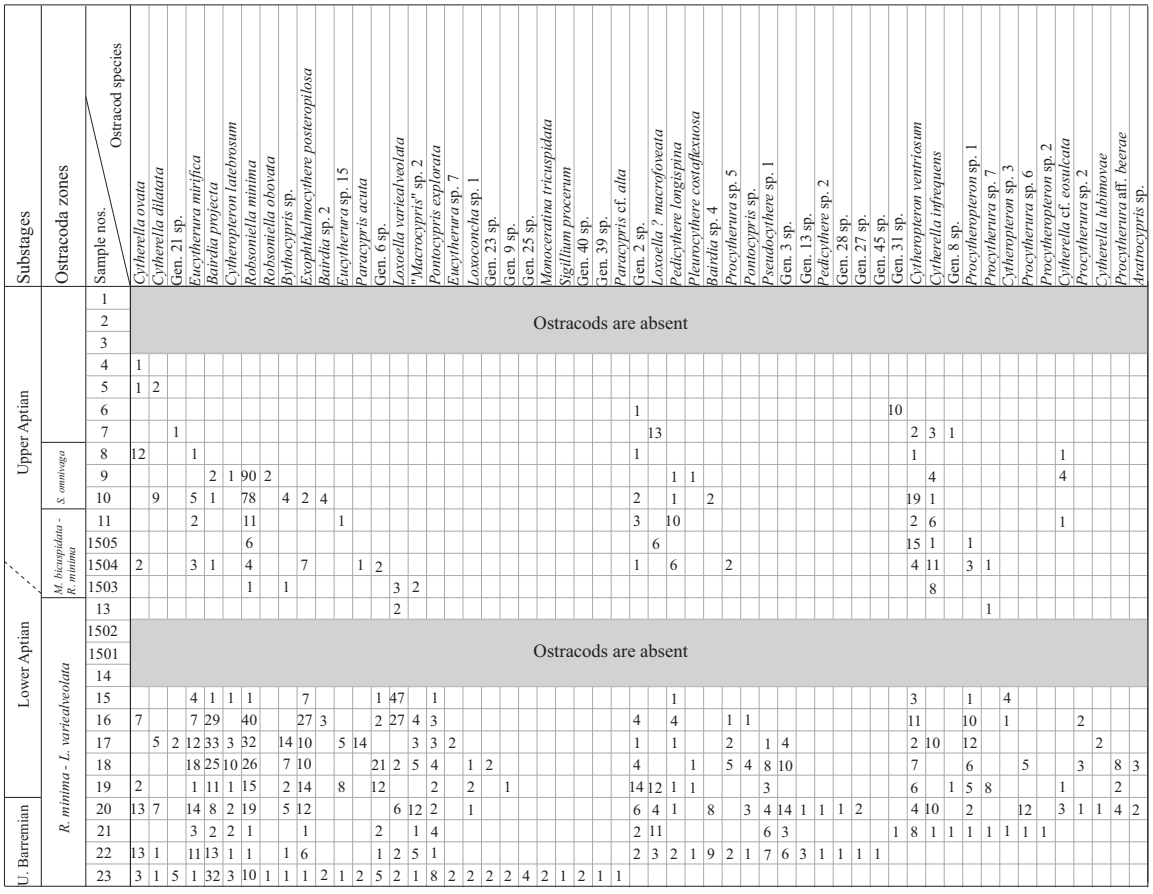

Table S4: The spores and pollens range chart of Zavodskaya balka section. Percentage of the amount spores and pollen.

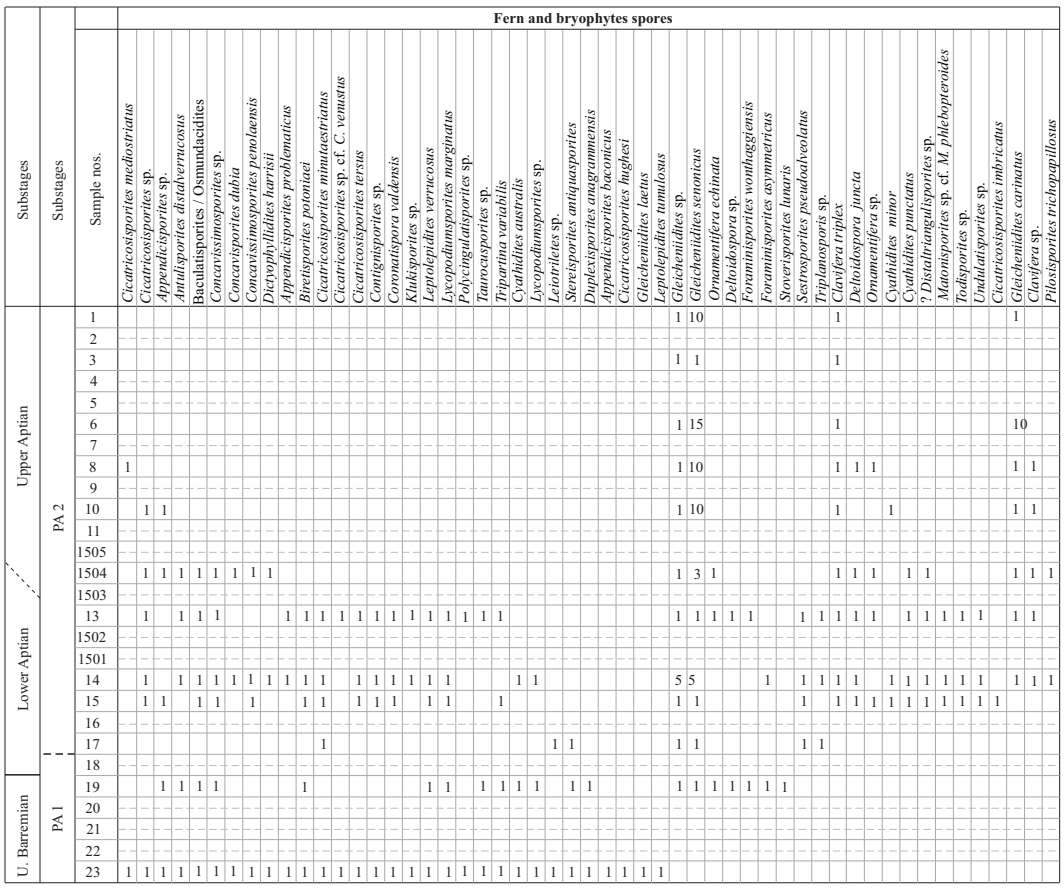

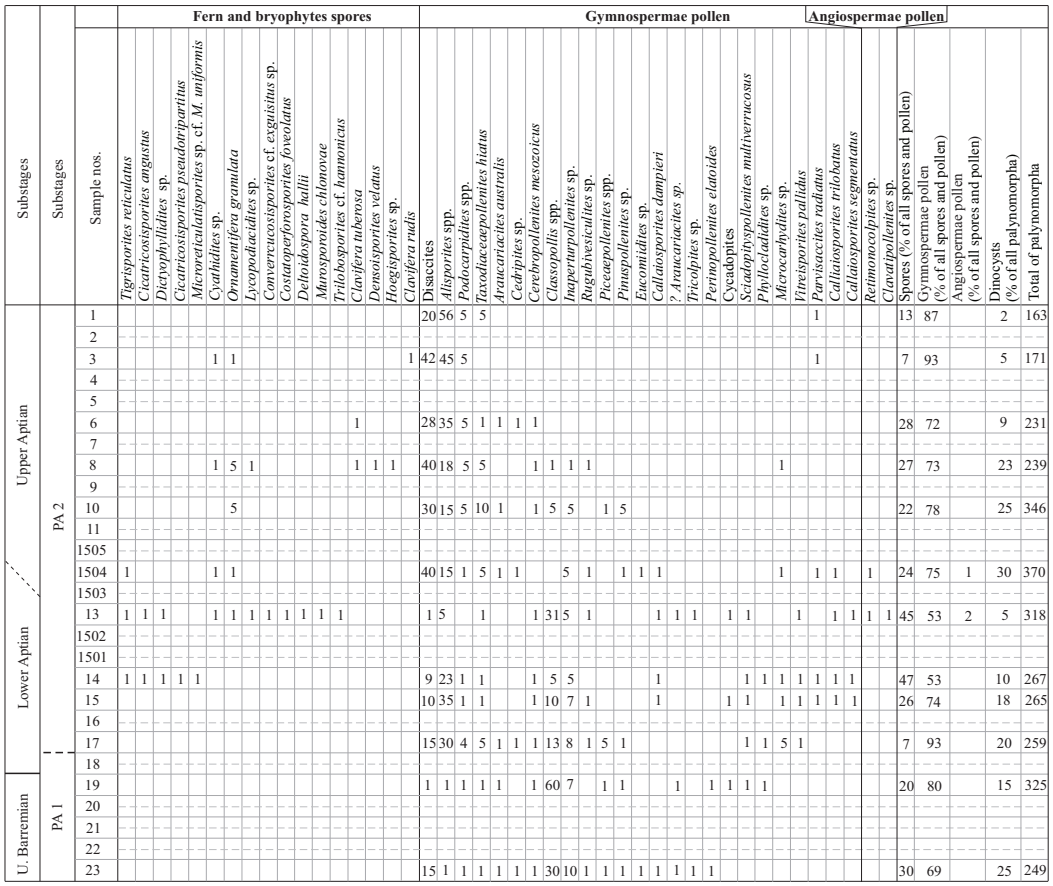

Table S5: The dinocyst range chart of Zavodskaya Balka section. Numbers are specimen abundance in the sample.

Substages	Upper Aptian													Lower Aptian								U. Barremian					
Substages	D 3							D 2														D 1					
Dinoflagellates species / Sample nos.	1	2	3	4	5	6	7	8	9	10	11	1505	1504	1503	13	1502	1501	14	15	16	17	18	19	20	21	22	23
Pterospermella sp.	1					2				1			1					1			1						1
Pterodinium spp.						2		8		16			8					1	3		3		4				2
Canningia colliveri								1																			2
Cerbia tabulata								1		9			10					1			1		1				3
Circulodinium distinctum								1		4			3		1				3		1						2
Cleistosphaeridium spp.								12		24			19					2	6		5		5				2
Cribroperidinium? cf. *edwardsii*								2		3																	1
Dingodinium? albertii								1		5			3						3		3		2				1
Oligosphaeridium? asterigerum								1		2			1						1		2		3				1
Oligosphaeridium complex								1					1					1					1				1
Rhynchodiniopsis fimbriata								1															1				1
Spiniferites spp.								4		11			34					3	9		3		6				6
Trichodinium sp.								1																			1
Chlamydophorella sp.										1								1									1
Coronifera oceanica										2			3								2		1				1
Cribroperidinium? cf. *muderogense*										1													1				1
Gardodinium eisenackii										1			4										1				2
Impagidinium alectrolophum													1										1				1
Kleithriasphaeridium eoinodes													1						1				1				1
Prolixosphaeridium parvispinum													5					1	1		1		1				1
Cribroperidinium sp.															2			1	2		1		1				1
Spiniferites dentatus																		1					1				4
Taleisphaera hydra subsp. *elongata*																		7					1				1
Ctenidodinium elegantulum																			1				1				1
Chytroesphaeridia sp.																			1								1
Dingodinium? cf. *spinosum*																					1						1
Circulodinium brevispinatum																											1
Circulodinium cf. *attadalicum*																											1
Circulodinium cf. *deflandrei*																											1
Cribroperidinium? cf. *cornutum*																											1
Cribroperidinium sepimentum																											1
Cyclonephelium cf. *intonsum*																											1
Pareodinia sp.																											1
Pilosidinium sp.																											1
Subtilisphaera ventriosa																											1
Surculosphaeridium sp. III																											1
Subtilisphaera perlucida			3			10		9		10			5		1			3	1		1		1				
Meiourogonyaulax stoveri								1		1			2										1				
Impagidinium verrucosum										1			1								1		1				
aff. *Valensiella reticulata*													27						1		1		1				
Tanyosphaeridium boletus																		1	1				1				
Florentinia sp.																			1		1		1				
M. cf. *staurota* sensu Dav., Verd., 1974																					1		1				
Achomosphaera sp.																							1				
Cyclonephelium sp.																							2				
Muderongia sp.																							1				
Pervosphaeridium cf. *truncatum*																							1				
Batiacasphaera sp.								2										1			1						
Odontochitina operculata								1		8			3					1			1						
Pseudoceratium polymorphum								1		1			1					1			2						
aff. *Wallodinium* sp.								1		2			2						1		1						
Oligosphaeridium sp.										1					1			1	1		1						
Palaeoperidinium cretaceum													1		2			1									
Protoellipsodinium cf. *clavulus*													1								2						
Pseudoceratium cf. *retusum*																		1			1						
? *Kalyptea* sp.																					1						
? *Kallosphaeridium* sp.																					1						
Pseudoceratium pelliferum																					1						
Oligosphaeridium albertense																					1						
Ovoidinium incomptum								3		5									3								
Apteodinium sp.										1									1								
Protoellipsodinium spinosum										3			1						1								
Cometodinium sp.																			1								
Hystrichosphaerina schindewolfii																			1								
Impagidinium sp.																			1								
Rhynchodiniopsis cf. *cladophora*																			1								
Fromea sp.																			1								
Surculosphaeridium sp.								1		6								1									
Exochosphaeridium phragmites													1		3			1									
Pseudoceratium securigerum													3					2									
Tasmanites sp.																		2									
Florentinia mantellii													4		1												
Protoellipsodinium spinocristatum	1		2			5				3			3														
Cassiculosphaeridia sarstedtensis								3		1			1														
Tehamadinium tenuiceras								1					1														
Heslertonia heslertonensis										1			1														
Callaiosphaeridium trycherium													1														
Cribroperidinium? tenuiceras													4														
Cribroperidinium cf. *conjunctum*													3														
Oligosphaeridium prolixispinosum													1														
Cribroperidinium boreas										1																	
Rhombodella paucispina										1																	
Florentinia cooksoniae								1																			
Pseudoceratium sp.								1																			
Cymatiosphaera sp.								1																			
phycomata green algae			13			3																					
indetermined fragment chorate cysts								6		24			8								3						13
acritarchs	1		2							5								1	1		1						3